

CONTROL OF BRUSHLESS DC MOTOR FOR SPEED CONTROL APPLICATION

A DISSERTATION SUBMITTED IN PARTIAL FULFILMENT OF THE
REQUIREMENTS FOR THE AWARD OF THE DEGREE OF

MASTER OF ENGINEERING

IN

CONTROL & INSTRUMENTATION

SUBMITTED BY
AMARNATH YADAV
(Roll NO. 8667)

UNDER THE ESTEEMED GUIDANCE

OF

Dr. Vishal Verma



**DEPARTMENT OF ELECTRICAL ENGINEERING
DELHI COLLEGE OF ENGINEERING
UNIVERSITY OF DELHI
2004-2006**

CERTIFICATE

It is certified that Mr. Amarnath Yadav, Roll No.8667, student of M.E, Control and Instrumentation, Department of Electrical Engineering, Delhi College of Engineering, has submitted the dissertation entitled “**Control of Brushless DC Motor for Speed Control Application**”, under my guidance towards partial fulfillment of the requirements for the award of the degree of Master of Engineering (Control & Instrumentation Engineering).

This dissertation is a bonafide record of project work carried out by him under my guidance and supervision. His work is found to be good and his discipline impeccable during the course of the project.

I wish him success in all his endeavors.

Date:

(Dr. Vishal Verma)

Assistant Professor

Deptt. of Electrical Engineering

Delhi College of Engineering

ACKNOWLEDGEMENT

I would like to avail this opportunity to humbly thank and appreciate the contribution and support, which various individuals have provided for the successful completion of this dissertation.

My heartfelt thanks to my project guide **Dr. Vishal Verma**, Assistant Professor, Department of Electrical Engineering, DCE, who provided me an opportunity to work under his guidance. His guidance and suggestions helped me to complete the project in this advanced field.

I extend my sincere thanks to **Dr. Parmod Kumar**, Professor & Head, Department of Electrical Engineering, DCE, whose constant admiration and encouragement made this work possible.

I would like to extend my sincere appreciation to **Mr. Mahesh Napa** for reviewing this report and providing valuable comments and thoughtful criticism.

I am indebted to my **parents and family** for their love and prayers.

Lastly, I thank Almighty GOD for his countless blessings.

DATE:

AMARNATH YADAV

College Roll No. 09/C&I/04

Delhi Univ. Roll No. 8667

ABSTRACT

Brushless DC motors have a permanent-magnet rotor, and the stator windings are wound such that the back electromotive force (EMF) is trapezoidal. It therefore requires rectangular-shaped stator phase currents to produce constant torque. The Motors possess high torque/weight ratio, operate at very high speed, are very compact and are electronically controlled. Due to absence of mechanical brushes they require lesser maintenance. It is therefore, they replacing DC motor in variable speed servo applications. The desired excitation of machine could be made possible due to the rapid developments made in the field of power electronics and power digital signal processors (DSPs).

In this dissertation, a e brushless DC motor drive system has been analyzed, designed, modeled, simulated and developed. A comprehensive mathematical modeling of brushless DC motor ,its drive system is developed using SIMULINK and sim-powersystem blockset under MATLAB environment The dynamic response of the BLDC drive under various operating conditions such as starting, speed reversal and load perturbation is presented to demonstrate to the effectiveness of the system under MATLAB environment using SIMULINK and sim-powersystem blockset.

The dynamic response of the BLDC drive is modeled for many closed loop speed controller. The considered closed loop speed controllers are proportional integral speed controller, fuzzy logic controller, hybrid controller and

fuzzy pre-compensated controller. A comparative study of the response of the BLDC drive is demonstrated with application of these speed controllers.

TABLE OF CONTENTS

	Page No.
CERTIFICATE	ii
ACKNOWLEDGEMENTS	iii
ABSTRACT	iv
LIST OF FIGURES	ix
LIST OF TABLES	xii
LIST OF SYMBOLS	xiii
CHAPTER-I INTRODUCTION	
1.1 General	1
1.2 Concept and Applications of Brushless DC Motor Based Drives	2
1.2.1 Basic control approach	4
1.3 Scope of Work	6
1.3.1 Closed loop performance of BLDC drive	7
1.3.2 Implementation of BLDC drive	7
1.4 Outline of Chapters	8
CHAPTER-II LITERATURE SURVEY	10
2.1 General	10
2.2 Literature Review	10
2.2.1 Electronic controlled brushless DC motor drives	11
2.3.2 Closed loop controllers	11
2.3.3 Speed estimation techniques for sensorless control	12
2.3 Conclusions	13

CHAPTER-III MODELLING OF BRUSHLESS DC MOTOR DRIVES	14
3.1 General	14
3.2 Operating Principle of the Proposed BLDC Drive	14
3.3 Description of BLDC Drive system	15
3.3.1 Speed controller	15
3.3.2 Limiter	17
3.3.3 Reference generator	17
3.3.4 Current controller	17
3.3.5 Voltage source inverter	18
3.3.6 Brushless DC motor	18
3.4 Modeling of the Drive System	18
3.4.1 Speed controllers	18
3.4.1.1 Proportional integral (PI) speed controller	19
3.4.1.2 Fuzzy logic controller	20
3.4.1.3 Hybrid controller	23
3.4.1.4 Fuzzy pre-compensated proportional integral controller	27
3.4.2 Modeling of position detection Unit	29
3.4.3 Modeling of reference current Generator	29
3.4.4 Modeling of PWM current controller	30
3.4.5 Modeling of Back Emf using rotor position	30
3.4.6 Modeling of PMBLDC motor and Inverter	31
3.5 Simulation of BLDC Drive System	32
3.5.1 Speed controllers	33

3.5.2	Reference generator	36
3.5.3	Hysteresis Controller and Inverter	36
3.5.4	Position Detection Unit	37
3.5.5	Brushless DC Motor	38
3.5.4	Complete System	39
3.6	Results and Discussions	39
3.6.1	Starting Dynamics	40
3.6.2	Reversal Dynamics	40
3.6.3	Load Perturbation	40
3.6.4	Response of Drive using Different Controllers	41
3.6.5	Comparative Study among different speed Controllers	63
3.7	Conclusions	64
CHAPTER-IV FUTURE SCOPE OF WORK		
4.1	General	66
4.2	Further scope of work	66
REFERENCES		68
APPENDIX		72
BIO-DATA		73

LIST OF FIGURES

Fig 1.1	Pattern of emf wave and current wave during operation
Fig 1.2	Switching sequence for three phase inverter feeding BLDC Motor
Fig.3.1	Basic Block Diagram of BLDC Drive System
Fig3.2	Basic structure of PI controller
Fig3.3	Basic Structure of Fuzzy Logic Controller
Fig3.4	Block diagram of Hybrid speed controller
Fig3.5	Pattern depicting contribution of component controllers in Hybrid Controller
Fig3.6	Block Diagram of Fuzzy pre-compensated PI controller
Fig3.7	Discrete PI controller
Fig3.8	Matlab model of Fuzzy logic controller
Fig3.9	Matlab model of Hybrid controller
Fig3.10	Matlab model of fuzzy pre-compensated model
Fig3.11	Matlab model of Reference generator
Fig3.12	Matlab model of Hysteresis controller with inverter
Fig3.13	Matlab model of position detection block
Fig3.14	Matlab model of BLDC motor
Fig3.15	Matlab model of complete BLDC drive system
Fig3.16	Three phase current under load perturbation for PI controller
Fig3.17	Back Emf produced under load perturbation for PI controller
Fig3.18	Phase 'a' current under load perturbation for PI controller
Fig3.19	Reference speed Vs real speed response under load Perturbation for PI controller
Fig3.20	Electromagnetic Torque produced under load perturbation for PI controller
Fig3.21	Three phase current under speed reversal for PI controller
Fig3.22	Back Emf produced under speed reversal for PI controller
Fig3.23	Phase 'a' current under speed reversal for PI controller
Fig3.24	Reference speed Vs real speed response under speed reversal for PI controller
Fig3.25	Electromagnetic Torque produced under speed reversal for PI controller
Fig3.26	Three phase current under load perturbation for Fuzzy controller

- Fig3.27 Back Emf produced under load perturbation for Fuzzy controller
- Fig3.28 Phase 'a' current under load perturbation for Fuzzy controller
- Fig3.29 Reference speed Vs real speed response under load Perturbation for Fuzzy controller
- Fig3.30 Electromagnetic Torque produced under load perturbation for Fuzzy controller
- Fig3.31 Three phase current under speed reversal for Fuzzy controller
- Fig3.32 Back Emf produced under speed reversal for Fuzzy controller
- Fig3.33 Phase 'a' current under speed reversal for Fuzzy controller
- Fig3.34 Reference speed Vs real speed response under speed reversal for Fuzzy controller
- Fig3.35 Electromagnetic Torque produced under speed reversal for Fuzzy controller
- Fig3.36 Three phase current under load perturbation for Hybrid controller
- Fig3.37 Back Emf produced under load perturbation for Hybrid controller
- Fig3.38 Phase 'a' current under load perturbation for Hybrid controller
- Fig3.39 Reference speed Vs real speed response under load perturbation for Hybrid controller
- Fig3.40 Electromagnetic Torque produced under load perturbation for Hybrid controller
- Fig3.41 Three phase current under speed reversal for Hybrid controller
- Fig3.42 Back Emf produced under speed reversal for Hybrid controller
- Fig3.43 Phase 'a' current under speed reversal for Hybrid controller
- Fig3.44 Reference speed Vs real speed response under speed reversal for Hybrid controller
- Fig3.45 Electromagnetic Torque produced under speed reversal for Hybrid controller
- Fig3.46 Three phase current under load perturbation for FPCPI controller
- Fig3.47 Back Emf produced under load perturbation for FPCPI controller
- Fig3.48 Phase 'a' current under load perturbation for FPCPI controller
- Fig3.49 Reference speed Vs real speed response under load perturbation for FPCPI controller

Fig3.50	Electromagnetic Torque produced under load perturbation for FPCPI controller
Fig3.51	Three phase current under speed reversal for FPCPI controller
Fig3.52	Back Emf produced under speed reversal for FPCPI controller
Fig3.53	Phase 'a' current under speed reversal for FPCPI controller
Fig3.54	Reference speed Vs real speed response under speed reversal for FPCPI controller
Fig3.55	Electromagnetic Torque produced under speed reversal for FPCPI controller
Fig3.56	Steady State Error of controllers
Fig3.57	Starting Response of controllers
Fig3.58	Undershoot on load application of controllers
Fig3.59	Overshoot on load removal of controllers

LIST OF SYMBOLS

E	Back EMF of the motor
i^*	Reference current
T_e	Instantaneous torque
ω_r	Angular velocity
i_a, i_b, i_c	Actual phase currents
i_a^*, i_b^*, i_c^*	Reference current for each phase
ω_r^*	Reference speed
T^*	Torque output from the controller
$\omega_{re(n)}$	Speed error at the n^{th} instant
$\omega_{r(n)}^*$	Reference speed at the n^{th} instant
$\omega_{r(n)}$	Actual speed at the n^{th} instant
K_p	Proportional gain
K_i	Integral gain
$T^*_{(n)}$	Torque command output from the controller at the n^{th} instant
$\Delta\omega_{re}$	Change in speed error
μ	Membership value
α	Output membership
$p(m)$	Location of peak of the membership function
W_{fl}	Weight of FL speed controller
W_{pi}	Weight of PI speed controller
T^*_{flk}	Torque output of the FL speed controller in the k_{th} region of the combination pattern
T^*_{pik}	Torque output of the PI speed controller in the k_{th} region of the combination pattern
ω_{r1}^*	Compensated reference speed
p	Differential operator
K_b	Back emf constant
θ_r	Rotor position
h_b	Hysteresis band
e_{an}	Back emf w.r.t neutral
$\lambda_a, \lambda_b, \lambda_c$	Flux linkages of each phase
R	Resistance per phase
M	Mutual inductance
L_s	Self inductance
B	Viscous friction coefficient
J	Inertia constant
P	Number of poles

LIST OF TABLES

Table 3.1	Rules for Fuzzy logic speed controller
Table 3.2	Rules for fuzzy pre-compensated system
Table 3.3	Reference current in each phase during every 60 deg of rotation
Table 3.4	Comparative Performance of Different Speed Controllers

CHAPTER-I

INTRODUCTION

1.1 General

The applications related to variable speed drives were dominated by DC motors for the last many decades. The prominence of DC motors in motion control is due to the easy controllability, stability and lesser requirement of semiconductor devices. Efforts have been made to replace them with AC motors due to many objections that arise from operational problems associated with the brush gear. The commutator speed is a limitation and noise, wear, RFI and environmental capability can be troublesome. The limitations of commutation and rotor speed in DC motors can overcome by the usage of induction or synchronous motors.

In the fractional and low integral-horsepower range the complexity of the AC drive is a drawback, especially when dynamic performance, high efficiency, and a wide speed range are among the design requirements. Therefore brushless DC motor form a better alternative in the range of 1- 10 KW. In this range brushless DC motor has better efficiency, torque per ampere, and effective power factor. Moreover, the power winding is on the stator where its heat can be easily removed, while rotor losses are extremely small. These factors combine to keep the torque /inertia ratio high in small motors. The brushless DC motors are easier to control, especially in its 'squarewave' configuration.

Rapid development in the field of power electronics has resulted in the availability of improved semiconductor devices (especially self commutating devices with high switching speeds, high current and voltage ratings) and compact circuits in modular form. Power digital signal processors have made the implementation of complex control schemes.

1.2 Concept and Applications of brushless DC Motor Drives

The permanent magnet brushless dc (BLDC MOTOR) motor is increasingly being used in computer, aerospace, military, automotive, industrial and household products because of its high torque, compactness, and high efficiency. The BLDC motor is inherently electronically controlled and requires rotor position information for proper commutations of current [1, 2]. Brushless dc motors have been put into practical use because of high efficiency and good controllability. A brushless dc motor requires an inverter and a position sensor to perform “commutation”. Three Hall sensors have been used as a position sensor for the brushless dc motor.

Fig 1.1 shows the operation of the brushless motor producing constants torque. The trapezoidal PMAC motor is specifically designed to develop nearly constant output torque when excited with six-step switched current waveforms of the type presented in the above figure. Trapezoidal PMAC motors are predominantly surface-magnet machines designed with wide magnet pole arcs and concentrated stator windings. The resulting back-EMF voltage induced in each

stator phase winding during rotation can be modeled quite accurately as a trapezoidal waveform as shown in below figure.

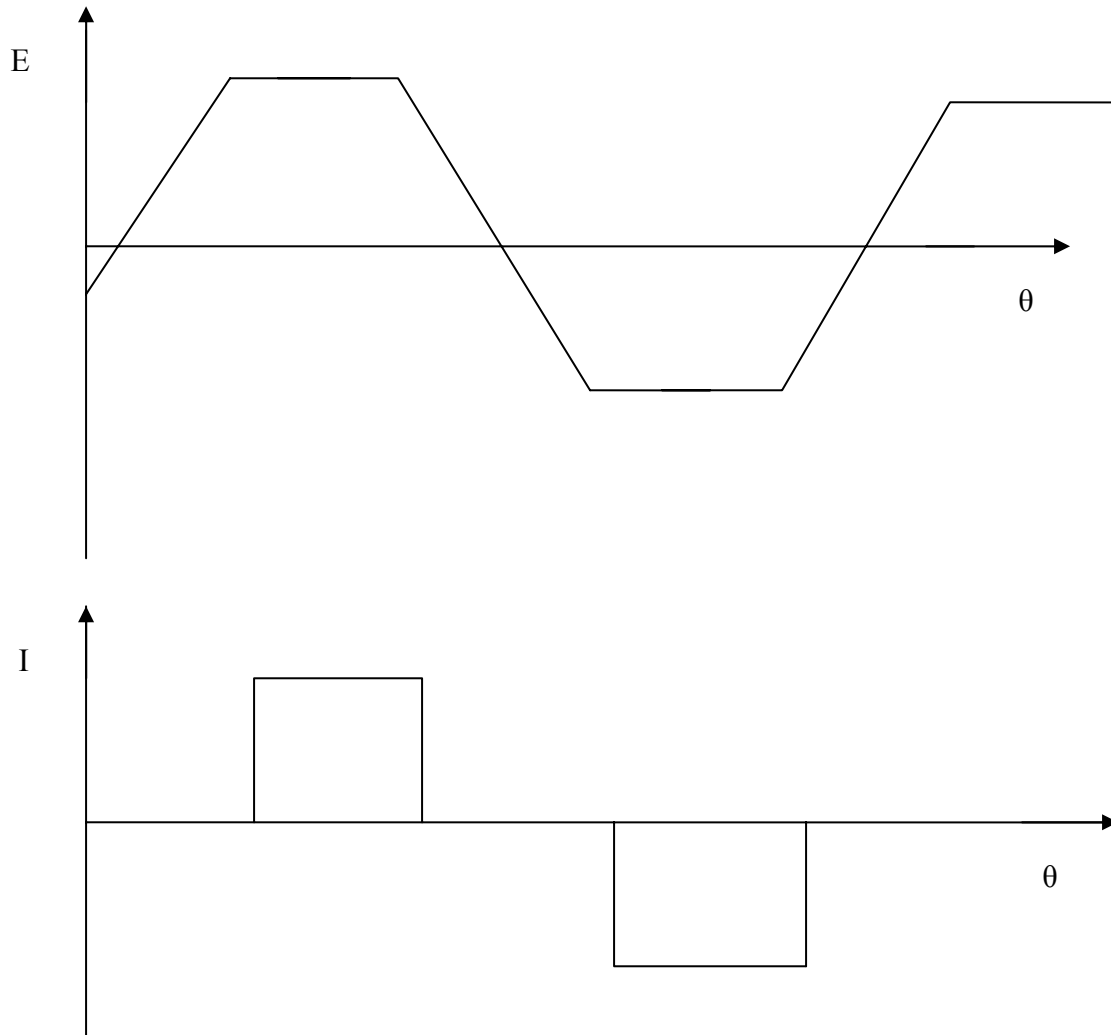


Fig 1.1 Pattern of emf wave and current wave during operation

The induced emf is proportional to the angular velocity of the motor. If a current with fixed amplitude is flowing into this machine phase during the time interval when the back-EMF is cresting as indicated in Fig.1.1, the instantaneous power converted by this phase from electrical form into mechanical form will be:

$$P = E \cdot I = T_e \cdot \omega_r; \tag{1.1}$$

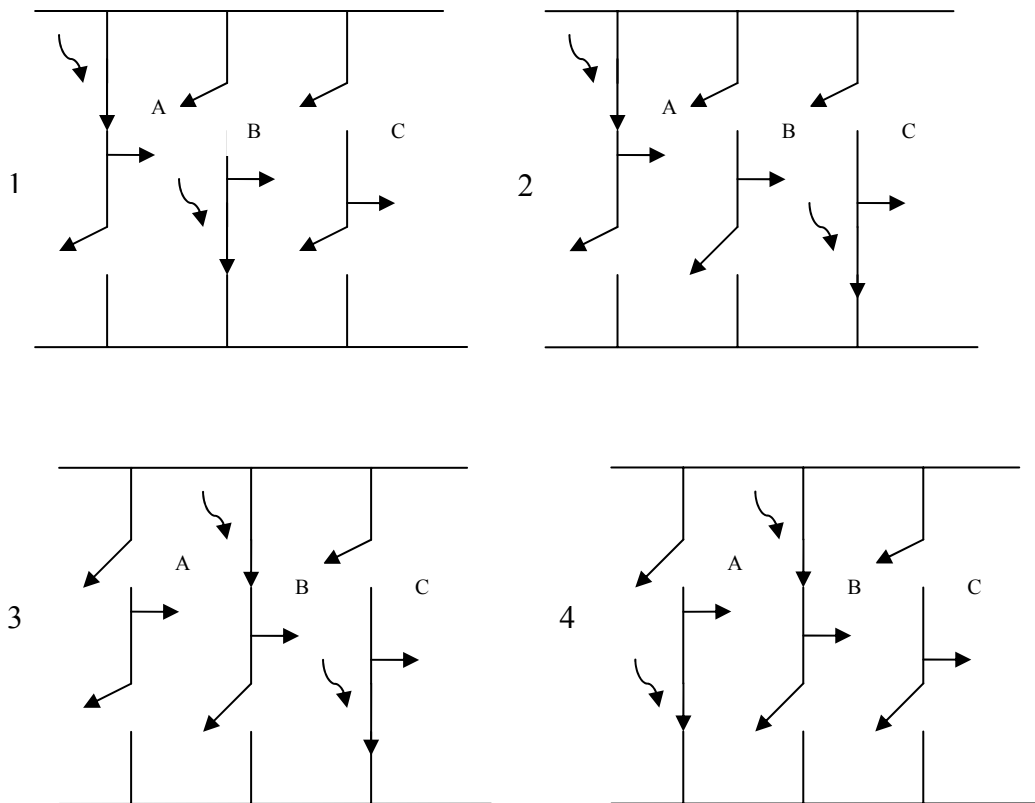
$$T_e = E \cdot I / \omega_r; \quad (1.2)$$

where T_e is the instantaneous torque developed by the excited phase, leading to 1.2. This torque equation is particularly significant since it indicates that the torque developed by the machine can be controlled very directly by varying the current amplitude. These dual direct proportionalities of back EMF to speed and torque to current expressed in (1.1) and (1.2) are identical in form to expressions characterizing a conventional dc motor with constant field excitation.

1.2.1 Basic control approach

The inverter which excites the trapezoidal PMAC has two primary responsibilities. *Electronic commutation* is the first of the two, requiring the inverter to direct excitation to the proper phases at each time instant in order to maintain synchronization and to maximize torque output. *Motor current regulation* is the second major inverter responsibility, taking advantage of the direct proportionality between current amplitude and output torque during self-synchronized operation. The electronic commutation function is accomplished by opening and closing the six inverter switches according to the six-step sequence shown in Fig. 1.2 to produce the phase-current excitation waveforms shown previously in Fig. 1.1. There are only six discrete inverter switching events during

each electrical cycle, and only two inverter switches--one in the upper inverter bank and one in the lower--are conducting at any instant, each for 120° elec. Under the assumption that the motor is connected in wye, this means that the inverter input current I , is flowing through two of the three motor phases in series at all times.



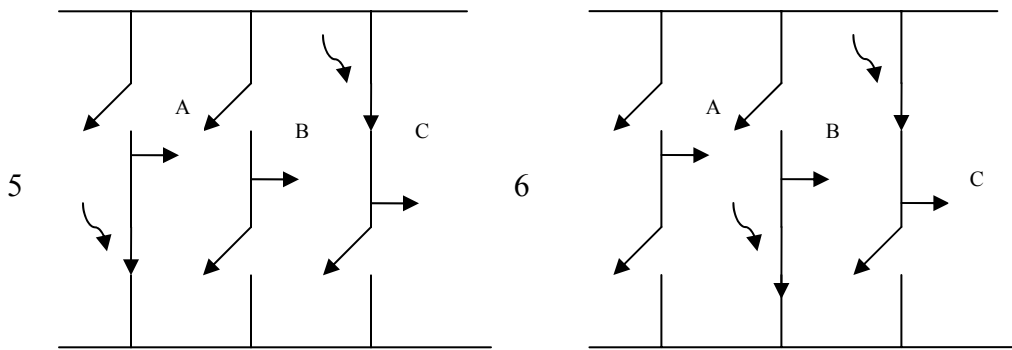


Fig 1.2 Switching sequence for three phase inverter feeding BLDC motor

Pulse width-modulation (PWM) control of one or both of two inverter switches which are “active” during each time interval shown in Fig. 1.2 is introduced to regulate the current flowing through the two energized motor phases. Although not included in Fig. 1.2, the free-wheeling diodes provide crucial conduction paths for the inductive motor phase currents whenever the inverter switches are turned off to accomplish PWM regulation or to transfer current to the next “active” motor phase. In essence, the switch-diode combinations in each of the three inverter phase legs form elementary switching converter modules which can regulate the inductive-motor phase-current amplitude in either direction.

1.3 Scope of work

The brushless DC motor drives exhibit quick starting response, fast reversal response and quick change over from one operating point to the other.

The BLDC motor drive can be operated in 180 deg or 120 deg squarewave conduction mode depending upon the magnetic arc length of the rotor.

The voltage source inverter (VSI) feeding the brushless DC motor is operated in the current controlled (CC) mode. The CC mode of VSI, lead to quick and fast response as the winding currents are regulated in accordance to mode of operation.

Improvement in the performance of BLDC motor drive is considered with different types of speed controllers. The speed controllers considered in his work are: proportional integral (PI) controller, fuzzy logic speed controller, hybrid of fuzzy logic speed controller and PI controller and fuzzy pre-compensated speed controllers. A comparative study has been carried out on the performance of the above speed controllers in BLDC motor drives.

The following research objectives have been identified to be investigated in this research work.

1.3.1 Closed loop performance of BLDC MOTOR drive

The main objective of the proposed investigation have been set on the improvement pf closed lop performance of the BLDC motor drive during transient and steady state operating points. The BLDC motor drive system is mathematically modeled in under and the various operating conditions namely starting, speed reversal and load perturbation in MATLAB using simulink and simpowersystem blockset. The simulation study has been carried out using the different speed controller such as proportional integral (PI) controller, hybrid speed controller, fuzzy logic controller and fuzzy pre-compensated speed controller.

1.3.2 Implementation of BLDC motor drive

The implementation of BLDC motor drive has been carried through minimum hardware development and software implementation in digital signal processor. The hardware development consists of the power circuits and the control circuit respectively. The control algorithm is developed in assembly language and implemented in the DSP(ADMC401).The pulse width modulated (PWM) signals emanated from the PWM channels of the DSP are fed to the six gate drivers inputs for the control of IGBT based VSI feeding a three-phase BLDC motor. Experiments have been carried out for various dynamic conditions such as starting, speed reversal, load application and load removal and the drive response has been recorded with different speed controllers.

1.4 Outline of chapters

The contents of the thesis have been divided in to the following chapters:

Chapter I

It includes the importance and potential applications of the BLDC MOTOR drive system. It also covers control techniques applied to the BLDC MOTOR drive system along with scope of proposed research work.

Chapter II

This chapter deals with an exhaustive literature review on the BLDC MOTOR drive system. It relates to the development in closed loop controllers. It includes the state of art on elimination of speed sensor and estimation of rotor speed by sensing the winding currents and dc link voltage.

Chapter III

This chapter deals with the modeling and simulation of BLDC MOTOR motor drive. It includes the simulation of the drive under various operating conditions, such as starting, speed reversal and load perturbation. A comparative study of different closed loop speed controllers has been made in terms of performance indices such as starting time, reversal time, and speed dip on load application, speed rise on load removal and steady state speed error on load

Chapter IV

This chapter includes the future scope of work.

CHAPTER II

LITERATURE SURVEY

2.1 GENERAL

The preceding chapter dealt with a general overview of control techniques, various potential applications of the brushless DC motor based drive system. The present chapter covers a literature review relating to various speed controllers based on soft computing (fuzzy logic, neural networks) and various methods to eliminate speed sensor from the drive system to reduce the system cost.

2.2 LITERATURE REVIEW

The brushless DC motors are now being increasingly applied in small KW drives (1-10Kw) due to their good dynamics. The upsurge in the application can be attributed to the rapid development made in the field of power electronics and microelectronics.

Thomas M. Jahns[19] gave a brief background of the permanent magnet machines. PMAC machine drives represent the convergence of at least two distinct threads of permanent-magnet machine development. One of these threads is the early development of line-start PMAC motors with embedded rotor squirrel cage windings designed for operation directly from utility supplied ac power. Work on this special class of PMAC machine dates back to the 1950's using Alnico magnets and continues today with modern magnet materials for direct line-start applications. Representing the second thread, permanent-magnet DC (PMDC) servo motors began to displace conventional wound-field DC motors in high-performance machine tool servo applications in the 1960's when solid-

state DC chopper circuits began to mature. Finally, in the 1970's, these two development paths converged as PMAC machines (without rotor cages) were combined with inverters to achieve high-performance motion control while eliminating the dual disadvantages of high rotor inertia and brush wear associated with PMDC motor commutators.

2.2.1 Electronic Controlled Brushless DC Motor Drives

P.C. Krause and S.D. Sudhoff [10] gave a detailed analysis of the 180 deg and 120 deg mode of operation of the drive system. The BLDC MOTOR motor drives are mainly fed from three phase full bridge inverter configuration but due to good dynamics and easy controllability, they are increasingly being applied to high volume applications. Such applications require the cost be as minimal as possible. R. Krishnan and Shiyong Lee [22] suggested a new converter topology (split supply) which requires lesser number of semiconductor switches. The models [11] proposed by pragasen pillay and R Krishnan approximated the EMF with trapezoidal waveform.

2.2.2 Closed Loop Controllers

The closed loop performance of the BLDC motor is largely dependent on the type of speed controller used. Traditionally PI controllers have been extensively used in the past many decades due to their lesser complexities and easy deployment. The tuning of the PI control is done on trial and error basis and they are very vulnerable to parameter variations.

The soft computing techniques like fuzzy logic and neural network are very promising as they are more robust than conventional non-linear controllers and

can handle the nonlinearities and parameter variation much better than the conventional controllers. M.A El-sharkawi ,A.A El-Samahy and M.L. El-Sayed[40] devised a multilayered neural network architecture for the identification and control of brushless DC motors operating in high performance drives environment.

To contain the ill-effects of the PI controller, many alternative controller configurations has been proposed. Fuzzy logic based pre-compensation techniques [37] exhibit superior performance when system is subjected to nonlinearities. Hybrid controllers [39], a combination of fuzzy logic and conventional PI controller extracts the best of both the controllers. The fuzzy logic provides a fast response and PI controller reduces the steady error.

2.3.3 Speed Estimation Techniques

The current flow in the windings of a brushless permanent-magnet (PM) machine must be synchronized to the instantaneous position of the rotor, and therefore, the current controller must receive information about the position of the machine's rotor. An auxiliary device (e.g., an optical encoder or resolver) may be used to measure rotor position, but there has been much interest in "sensorless" [24, 28, 29, 30, 31, 33] schemes, in which position information is derived by on-line analysis of the voltages and currents in the machine windings.

The inclusion of Hall sensors for speed detection makes the system lesser reliable and increases the cost of the system. Much of the recent work has been focused on the techniques to make the drive system *sensorless*. The

measurement of back-emf provides the rotor position as the magnitude of the voltage is proportional to angular velocity [14, 15, 16]. But at very low speed or during starting, the magnitude of the EMF is very low which makes this method suitable for certain speed range. Moriera [27] introduced an improved method for position sensing using motional EMF, which utilizes the third-harmonic component in the EMF waveform of a trapezoidal PM machine, and thus reduces the phase-shifting problem outlined above. Nesimi Ertugrul and Paul Acamley [4] came with a new algorithm based on flux linkage and current.

Tae-Hyung Kim, Byung-Kuk Lee, and Mehrdad Ehsani [28] presented a novel technique which measured speed from near zero to full speed.

2.3 CONCLUSIONS

The exhaustive literature review has revealed that research work carried out on BLDC motor based drives is largely influenced by the technical developments in power electronics, microelectronics and control systems. Most of the developments in these fields are in the direction reducing the hardware by introducing high-speed digital signal processors and reducing the sensing requirement for the drive system. Further work is directed towards further increasing the range of sensorless position detection algorithm.

CHAPTER III

ANALYSIS AND MODELLING OF BRUSHLESS DC MOTOR DRIVE

3.1 GENERAL

The concepts, electronic control technique, industrial applications of BLDC motor drives and an exhaustive literature review including various sensorless techniques were covered in the preceding chapters. The current chapter deals with modeling and simulation of the BLDC motor drive under various operating conditions.

The BLDC motor is fed from a current controlled voltage source inverter. Two feedback signals namely, one current and speed are used in BLDC motor drive system. An elaborate model of BLDC motor drive has been developed to simulate and focus on the drive response for starting, speed reversal and load perturbation for different closed loop speed controllers.

3.2 OPERATING PRINCIPLE OF THE PROPOSED BLDC MOTOR DRIVE SYSTEM

Fig 3.1 shows the basic building block diagram of BLDC motor drive. The control system consists of an outer speed feedback loop and an inner current feedback loop. Two of the three-phase current signals along with the speed signal are sensed and are used as feedback signals. The speed (ω_r) of the motor is compared to the reference speed (ω_r^*) and the error (ω_{re}) is processed in the speed controller. A limit is kept on the output of the speed controller depending

upon maximum permissible torque developed by the motor. The output of the speed controller (T) after limiting is considered as the reference torque (T^*).

The reference generator generates a reference signal for each of the phase. To generate the reference signals, it requires the position of the rotor which is supplied by the Theta generation block (Integrator).

The feedback current signals and the reference signals are fed in to the current controller. The error between the actual currents and the reference currents are used as modulating signals. The output from the current controller is used for gating the switches of the inverter.

3.3 DESCRIPTION OF THE BLDC MOTOR DRIVE SYSTEM

Fig 3.1 shows the structure of BLDC MOTOR drive. It consists of the speed controller, the reference generator, the PWM/Hysteresis controller, the voltage source inverter and the three phase brushless DC motor. The functions of these blocks are described in the following sections.

3.3.1 Speed Controller

The desired speed reference value (ω_r^*) is compared with the actual speed (ω_r) and the error is processed in the speed controller. The output of the speed controller is the control signal for the torque command (T^*). The different speed controllers namely, the proportional integral (PI) controller, the fuzzy logic controller, the hybrid controller and the fuzzy pre-compensated controller are used in BLDC MOTOR drive.

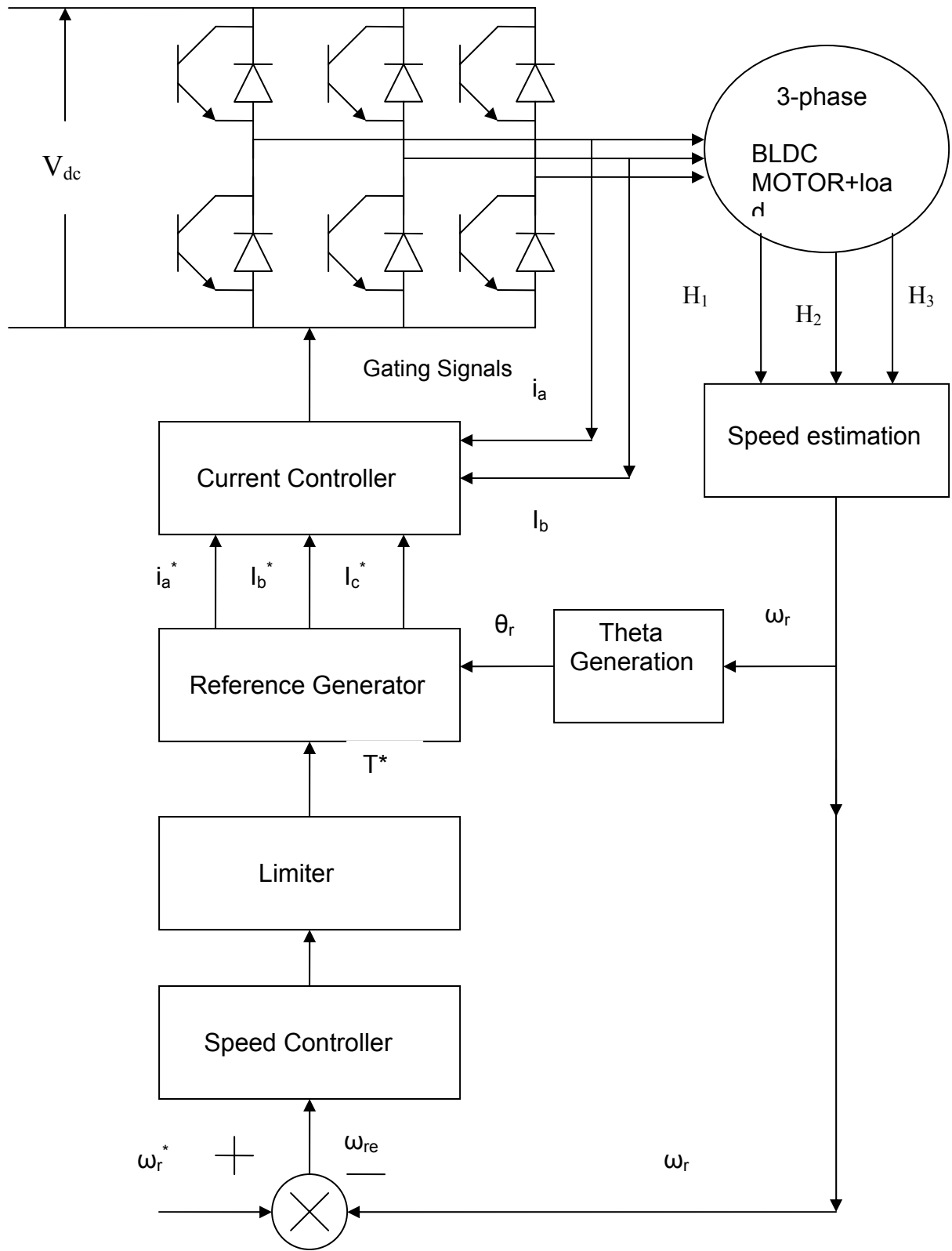


Fig.3.1 Basic Block Diagram of BLDC MOTOR Drive System

3.3.2 Limiter

When the drive operates in the transient conditions such as starting, reversing or load application, the speed controller output is very high value to achieve the steady state condition of the drive as fast as possible. As a result, the controller output signal (T^*) may become quite high and in some cases it may become higher than the breakdown torque of the motor. This may drive the motor towards instability. In order to avoid such circumstances, it becomes necessary to apply a certain limit on the output of the speed controller. As a result, the limit on the torque also ensures over current protection to the drive. Whenever reference speed changes or there is an application of load torque on the motor shaft, the speed controller output is limited to a maximum permissible value (T^*). Therefore, the limiter on the speed controller output provides an inherent stability to the closed speed control system.

3.3.3 Reference Generator

The function of the reference generator produces a reference signal for each of the three phases at each 60° rotation of the rotor. For this, it requires the rotor position. The input to the block is the command torque (T^*).

3.3.4 Current Controller

In the current controller, the power transistors are switched off and on, in accordance to whether the current is greater or less than the reference current. The error is used directly to control the states of the power transistors. This type controllers are called hysteresis controller. The hysteresis controller is used to limit the phase current within a preset hysteresis band. As the supply voltage is fixed, the switching frequency varies as the current error varies.

3.3.5 Voltage Source Inverter

The three-phase voltage source inverter comprises of a bridge configuration of six IGBT switches with respective free wheeling diode. Hysteresis controller operates the VSI in current control mode. The input to the VSI is constant DC voltage.

3.3.6 Three Phase Brushless DC motor

The Brushless DC motor behaves as DC motor, producing constant torque, when operated. The motor runs at the desired reference speed (ω_r) in the required direction and converts the electrical energy to mechanical energy.

3.4 MODELLING OF THE BLDC MOTOR DRIVE SYSTEM

Each component of the BLDC MOTOR drive system is modeled by a set of mathematical equations. Such a set of equations when combined together represent the mathematical model of the complete system. The modeling of different components of the drive system is as follows:

3.4.1 Speed Controller

Four different types of speed controllers have been considered for BLDC MOTOR drive.

The speed error (ω_{re}) is computed and used as an input to the speed controller, which outputs torque value (T). This value of torque (T) is fed to the limiter and the final reference torque (T^*) is obtained from the limiter. The speed error at the n^{th} instant of time is given as:

$$\omega_{re(n)} = \omega_{r(n)}^* - \omega_{r(n)} \quad (3.1)$$

where $\omega_{r(n)}^*$: reference speed at the n^{th} instant, $\omega_{r(n)}$: rotor speed at the n^{th} instant, $\omega_{re(n)}$: speed error at the n^{th} instant.

3.4.1.1 Proportional integral (PI) speed controller

The general block diagram of the PI speed controller is shown in Fig.3.2. The output of the speed controller at the n^{th} instant is given as:

$$T(t) = K_p e(t) + K_i \int e(t) dt \quad \text{continuous domain} \quad (3.2)$$

$$T_{(n)} = T_{(n-1)}^* + K_p \{ \omega_{re(n)} - \omega_{re(n-1)} \} + K_i \omega_{re(n)} \quad \text{Discrete domain} \quad (3.3)$$

Where K_p and K_i are the proportional and integral gain parameters of the PI speed controller. The gain parameters are judiciously selected by observing their effects on the response of the drive. Numerical values of the controller gains are given in the Appendix-I for the motor drive systems used in this investigation.

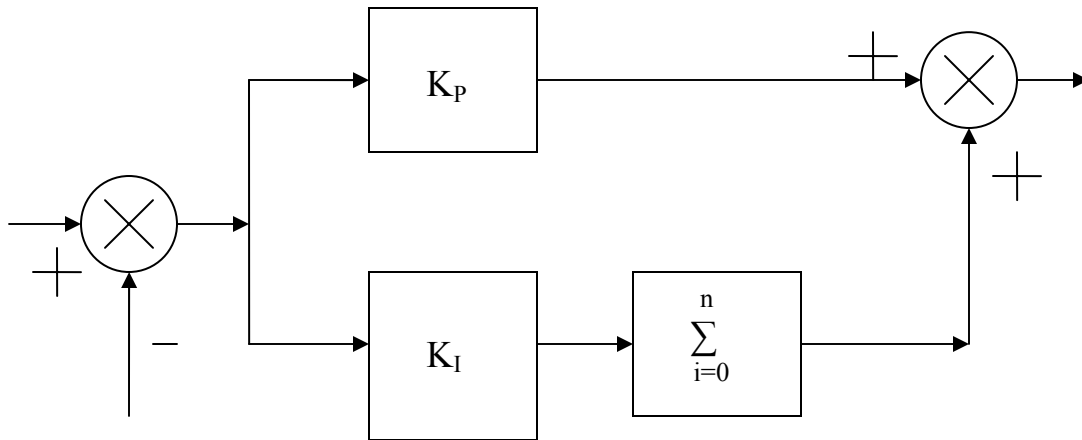


Fig 3.2 Basic structure of PI controller

3.4.1.2 Fuzzy logic speed controller

Fig.3.3 shows the basic configuration of an FLC, which comprises four principal components: a fuzzification interface, a knowledge base, decision making logic, and a defuzzification interface.

1) The fuzzification interface involves the following functions:

- measures the values of input variables,
- performs a scale mapping that transfers the range of values of input variables into corresponding universe of discourse, performs the function of fuzzification that converts input data into suitable linguistic values which may be viewed as labels of fuzzy sets.

2. The knowledge base comprises knowledge of the application domain and the attendant control goals. It consists of a “database” and a “linguistic (fuzzy) control rule base:”

- The database provides necessary definitions, used to define linguistic control rules and fuzzy data manipulation in an FLC,
- b) The rule base characterizes the control goals and control policy of the domain experts by means of a set of linguistic control rules.

3. The decision making logic is the kernel of an FLC, it has the capability of simulating human decision making based on fuzzy concepts and of inferring fuzzy control actions employing fuzzy implication and the rules of inference in fuzzy logic.

4. The defuzzification interface performs the following functions:

- a scale mapping, which converts the range of values of output variables into corresponding universe of discourse,
- b). defuzzification, which yields a non fuzzy control action from an inferred fuzzy control action.

The fuzzification interface converts crisp data into linguistic format. The decision maker decides in linguistic format with the help of logical linguistic rules supplied by the rule base and relevant data supplied by the database. The output of decision maker passes through the defuzzifier wherein the linguistic format signal is converted back to numeric form or crisp form. The decision making block uses the rules in the format of “if---then---else”. The fuzzy rules are stated in Table 3.1.

In accordance to the fuzzy logic concept, the processing takes place as follows:

- Calculation of n^{th} instant values of the two input signals namely, speed error and change in speed error

$$\omega_{re}(n)=\omega_r^*(n)-\omega_r(n) \quad (3.4)$$

$$\text{Changeoferror } (\Delta\omega_{re})=\omega_{re}(n)-\omega_{re}(n-1) \quad (3.5)$$

Where $\omega_{re}(n)$: speed error at the n^{th} instant ; $\Delta\omega_{re}$: change in speed error.

- Scaling of the two input signals namely, speed error and change in speed error
- The scaled input signals are fed to the fuzzy logic controller
- The scaled crisp data is converted to linguistic format in accordance with the defined fuzzy sets.
- In accordance to the linguistic rules, value of the output signal is determined. The required rules and data are supplied by the rule base and the database.
- The linguistic output is converted back into crisp output data by application of the method of defuzzification as follows:

Given a combination of two inputs, the membership of the corresponding output is taken as minimum membership value of the two respective inputs.

Mathematically,

$$\alpha=\min[\mu(\text{input1}),\mu (\text{input2})] \quad (3.6)$$

$$\text{Crispvalue}=\{\sum p(m) \alpha\} / \sum \alpha \quad (3.7)$$

Where μ refers to membership value, the output membership is stored in α and $p(m)$ refers to location of peak of the membership function. The crisp value obtained is re-scaled back to get the controller output, which is considered as the reference torque (T^*).

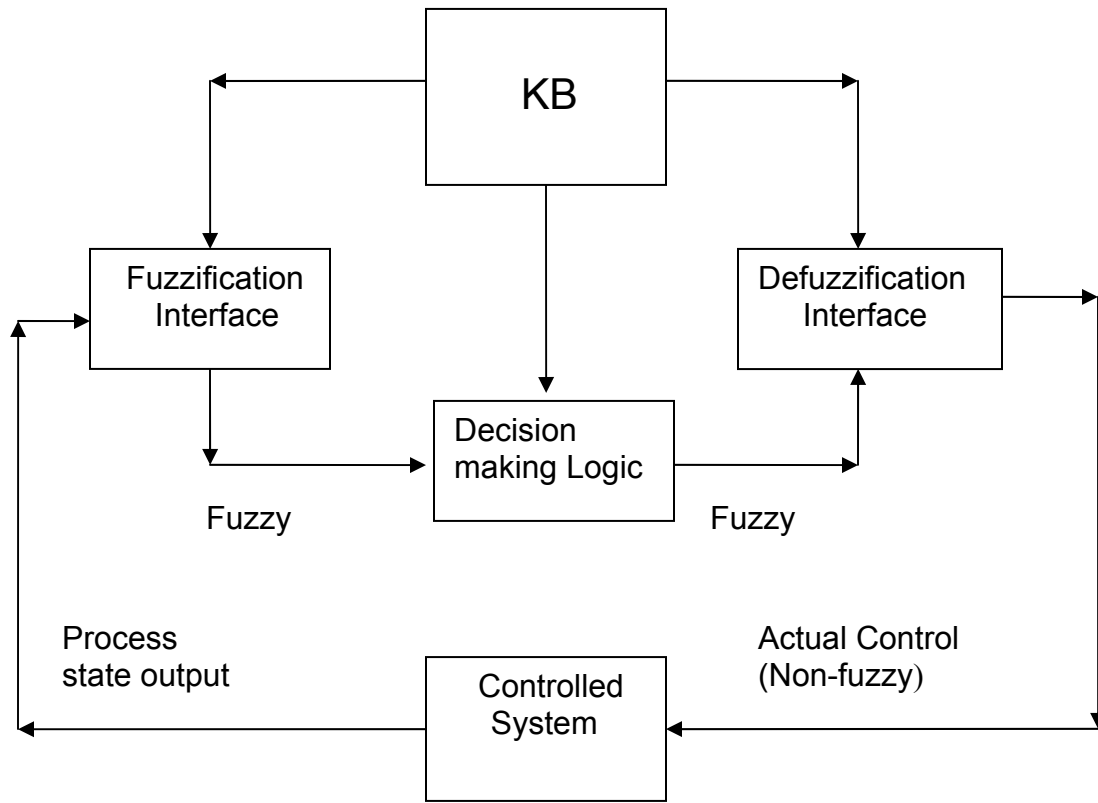


Fig 3.3 Basic Structure of Fuzzy Logic Controller

3.4.1.3 Hybrid speed controller

FLC appears very useful when the processes are too complex for analysis by conventional quantitative techniques or when the available sources of information are interpreted qualitatively, inexactly, or uncertainly. The BLDC MOTOR drive considered here is highly non-linear and the conventional techniques do not fulfill this purpose. In such cases, FLC appears to be a good alternative. The major disadvantage in this type of control logic is the presence of steady error on load.

CE	E	NB	NM	NS	ZE	PS	PM	PB
NB	NB	NB	NB	NB	NM	NS	ZE	
NM	NB	NB	NM	NM	NS	ZE	PS	
NS	NB	NM	NS	NS	ZE	PS	PM	
ZE	NB	NM	NS	ZE	PS	PM	PB	
PS	NM	NS	ZE	PS	PS	PM	PB	
PM	NS	ZE	PS	PM	PM	PB	PB	
PB	ZE	PS	PM	PB	PB	PB	PB	

Table 3.1 Rules for Fuzzy logic speed controller

To eliminate this disadvantage it is necessary to combine FL control with another suitable control technique, which is capable of removing the disadvantage existing in FL control. Therefore, a PI controller is used in combination with FL such that at the operating point the PI controller takes over eliminating the disadvantage of FL controller. Similarly, when away from the operating point FL controller dominates and eliminates the errors due to PI controller such as occurrence of overshoot and undershoot in drive response. Such a speed controller where weighted combinations of two controller outputs

contribute to the net output is called hybrid speed controller. Fig 3.6 shows the block diagram of such controller.

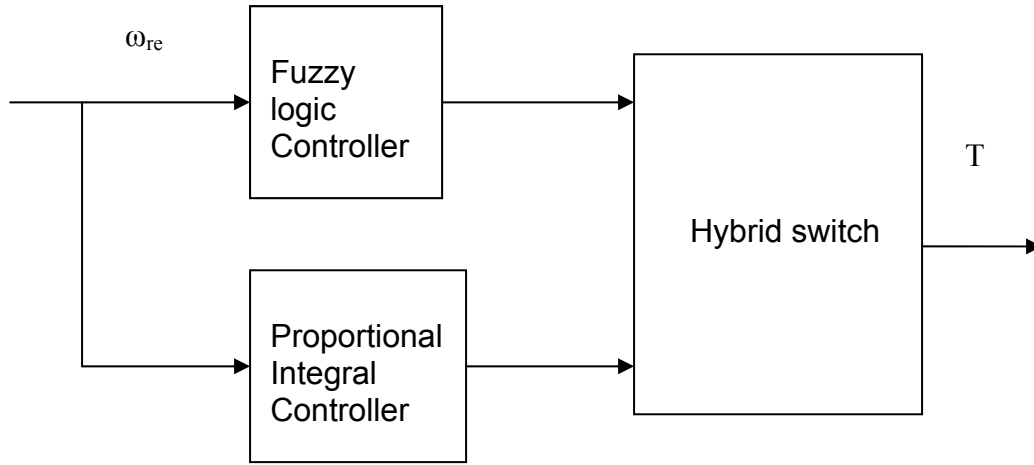


Fig 3.4 Block diagram of Hybrid speed controller

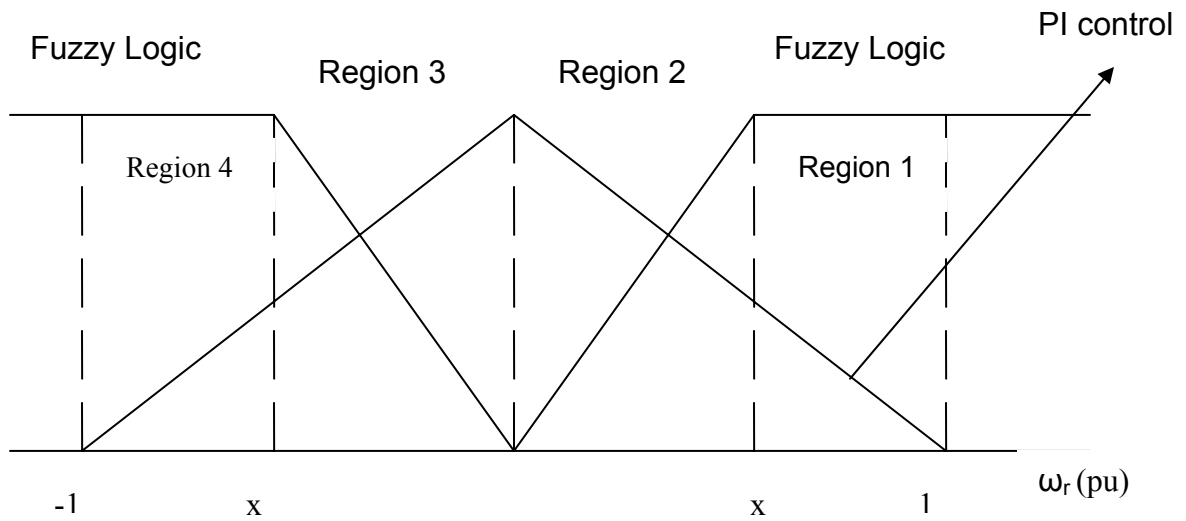


Fig 3.5 Pattern depicting contribution of component controllers in Hybrid Controller

Fig 3.5 shows the pattern for combining the outputs of PI and FL speed controllers respectively as a function of speed error (pu) scaled within a suitable range. At the operating point, the PI controller becomes predominant and when away from the operating point, the FL controller becomes dominant. The net output of the hybrid speed controller is a weighted sum of PI and FL speed controller outputs. Respective weightage

Controller is a weighted sum of PI and FL speed controllers towards the net output and is calculated as follows:

Region A: Speed error between x pu and 1.0 pu.

$$W_{fl}=1.0 \quad (3.8)$$

$$W_{pi} = 1- \omega_{re(pu)} \quad (3.9)$$

Region B: Speed error between 0.0 pu and x pu

$$W_{fl} = (1/x) \omega_{re(pu)} \quad (3.10)$$

$$W_{pi} = 1- \omega_{re(pu)} \quad (3.11)$$

Region C: Speed error between -x pu and 0.0 pu

$$W_{fl} = (-1/x) \omega_{re(pu)} \quad (3.12)$$

$$W_{pi} = 1+ \omega_{re(pu)} \quad (3.13)$$

Region D: Speed error between -1.0 pu and -x pu

$$W_{fl} = 1.0 \quad (3.14)$$

$$W_{pi} = 1+ \omega_{re(pu)} \quad (3.15)$$

where W_{fl} refers to the weight of FL speed controller , W_{pi} refers to the weight of PI speed controller , $\omega_{re(pu)}$ refers to the speed error in pu scale.

The net torque output of the hybrid speed controller is expressed as:

$$T_k = W_{flk} T_{flk}^* + W_{pik} T_{pik}^* \quad (3.16)$$

T_{flk}^* refers to the torque output of the FL speed controller (after application of speed limit) in the k_{th} region of the combination pattern, T_{pik}^* refers to the torque output of the PI speed controller (after application of speed limit) in the k_{th} region of the combination pattern and T_k refers to the output torque of the hybrid speed controller from the k_{th} region of the combination pattern fed to the limiter.

3.4.1.4 Fuzzy pre-compensated proportional integral (FPPI) speed controller

The PI controller has been around for many years due to its simple structure and ease of application. But it exhibits poor performance when subjected to parameter variations as well as the problems of undershoot and overshoot occurrence. A pre-compensation based on fuzzy logic is applied to the reference signal to make it more effective under such circumstances. As a result, depending upon the value of speed error (ω_{re}) and change in speed error ($\Delta\omega_{re}$), the FI control produces a signal u , which may be positive or negative. The algebraic addition of the FI controller output (u) with the defined reference speed (ω_r^*) produces the pre-compensated reference speed (ω_{r1}^*) to be used as reference speed in the remaining control action of PI controller.

Fig 3.6 shows the schematic block diagram of FPPI speed controller. The fuzzy rules are stated in Table 3.2. The control algorithm takes place as follows:

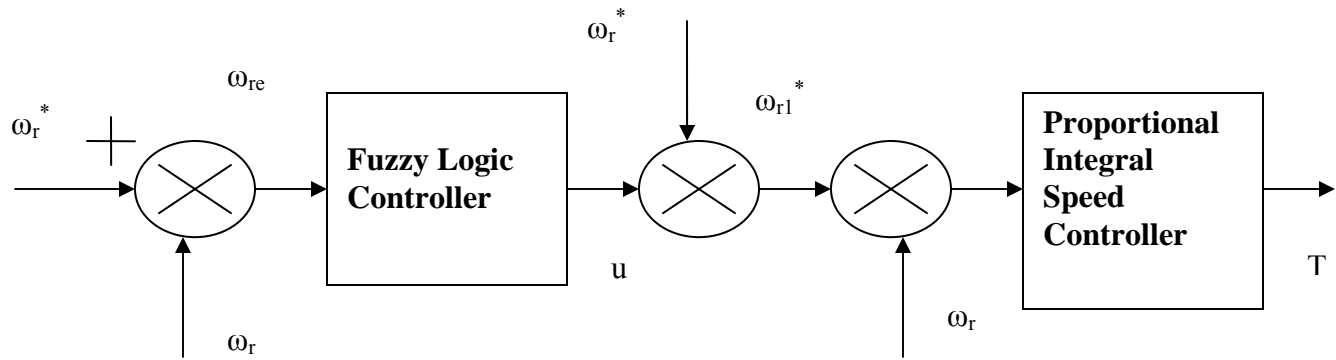


Fig 3.6 Block Diagram of Fuzzy pre-compensated PI controller

E \ E	NB	NM	NS	ZE	PS	PM	PB
CE							
NB			NB	NB	NB		
NM	NB	NB	NB	NB	NB	NB	NB
NS	NB		NS	NM	NM	NM	PM
ZE	NB	NM	NS	ZE	PS	PM	PB
PS	NM	PM	PM	PM	PM		PB
PM	PB	PB	PB	PB	PB	PB	PB
PB			PB	PB	PB		

Table 3.2 Rules for fuzzy pre-compensated system

3.4.2 Modeling of Position Detection Unit

The position (θ_r) of the rotor is determined through the angular velocity(ω_r).

$$\omega_r = p(\theta_r) \quad (3.17)$$

p =time differential operator

3.4.3 Modeling of Reference Current Generator

The magnitude of the three phase current I^* is determined by using reference torque T^* and the back emf constant K_b as $I^*=T^*/K_b$. Depending on the rotor position, the reference current generator block generates three-phase reference currents i_a^* , i_b^* , i_c^* by taking the value of reference current magnitude as I^* , $-I^*$ and zero.

Rotor Position Signal	Reference Currents		
θ_r	i_a^*	i_b^*	i_c^*
0-60	I^*	$-I^*$	0
60-120	I^*	0	$-I^*$
120-180	0	I^*	$-I^*$
180-240	$-I^*$	I^*	0
240-300	$-I^*$	0	I^*
300-360	0	$-I^*$	I^*

Table 3.3 Reference current in each phase during every 60 deg of rotation

These reference currents are fed to the PWM current controller.

3.4.4 Modeling of PWM Current Controller

The PWM current controller contributes to the generation of the switching signals for the inverter devices. The switching logic is formulated as given below.

If $i_a < (i_a^* - h_b)$ switch 1 ON and switch 4 OFF

If $i_a > (i_a^* + h_b)$ switch 1 OFF AND switch 4 ON

If $i_a < (i_a^* - h_b)$ switch 3 ON and switch 6 OFF

If $i_a > (i_a^* + h_b)$ switch 3 OFF and switch 6 ON

If $i_a < (i_a^* - h_b)$ switch 5 ON and switch 2 ON

If $i_a > (i_a^* + h_b)$ switch 5 OFF and switch 2 ON

Where, h_b is the hysteresis band around the three phase reference currents

3.4.5 Modeling of Back Emf Using Rotor Position

The phase back emf in the PMBLDC MOTOR motor is trapezoidal in nature and is function of the speed (ω_r) and rotor position angle (θ_r) as shown in Figure 2.

The normalized function of back emfs is shown in Figure 3. From this, the phase back emf e_{an} can be expressed as:

$$e_{an} = E \qquad 0 < \theta_r < 120 \qquad (3.18)$$

$$e_{an} = (6 \cdot E / \pi) \cdot (\pi - \theta_r) - E \qquad 120 < \theta_r < 180 \qquad (3.19)$$

$$e_{an} = -E \qquad 180 < \theta_r < 300 \qquad (3.20)$$

$$e_{an} = (6 \cdot E / \pi) \cdot (\theta_r - 2 \cdot \pi) + E \qquad 300 < \theta_r < 360 \qquad (3.21)$$

Where, $E = K_b \cdot \omega_r$. The back emf function of other two phases e_{bn} and e_{cn} are defined in similar way using E and θ_r .

3.4.6 Modeling of PMBLDC MOTOR Motor And Inverter

The PMBLDC MOTOR motor is modeled in the 3-phase abc variables. The general volt ampere equation for the circuit can be expressed as :

$$v_{an}=R*i_a+p\lambda_a+e_{an}; \quad (3.22)$$

$$v_{bn}=R*i_b+p\lambda_b+e_{bn}; \quad (3.23)$$

$$v_{cn}=R*i_c+p\lambda_c+e_{cn}; \quad (3.24)$$

where v_{an} , v_{bn} , v_{cn} are phase voltages.

p =time differential operator

R =resistance per phase.

The λ_a , λ_b , λ_c are total flux linkages of phase windings a, b, and c respectively.

Their values can be expressed as;

$$\lambda_a = L_s * i_a -M(i_b+ i_c); \quad (3.25)$$

$$\lambda_b = L_s * i_b -M(i_a+ i_c); \quad (3.26)$$

$$\lambda_c = L_s * i_c -M(i_a + i_b); \quad (3.27)$$

where L_s and M are the self and mutual inductances respectively.

The PMBDLC motor has no neutral connection and hence this results in:

$$i_a+i_b+i_c=0 \quad (3.28)$$

after substitution of eq (11) in esq. (8),(9),(10),we get

$$\lambda_a = i_a *(L_s+M)$$

$$\lambda_b = i_b*(L_s +M)$$

$$\lambda_c = i_c *(L_s +M)$$

final equations after substitution are

$$p(i_a) = 1/(L_s + M) * (v_{an} - R * i_a - e_{an}) \quad (3.29)$$

$$p(i_b) = 1/(L_s + M) * (v_{bn} - R * i_b - e_{bn}) \quad (3.30)$$

$$p(i_c) = 1/(L_s + M) * (v_{cn} - R * i_c - e_{cn}) \quad (3.31)$$

The developed electromagnetic torque is expressed as

$$T_e = (e_{an} * i_a + e_{bn} * i_b + e_{cn} * i_c) / \omega_r \quad (3.32)$$

Where ω_r is rotor speed in rad/s

The mechanical equation of motion in speed derivative can be expressed as

$$p(\omega_r) = (P/2)(T_e - T_l - B * \omega_r) / J \quad (3.33)$$

where P is no of poles, T_l is the load torque in N-m, B is the frictional coefficient in N-m/rad, and J is the moment of inertia in Kg-m².

The derivative of the rotor position

$$p(\theta_r) = \omega_r \quad (3.34)$$

The set of differential equations mentioned above describe the developed model in terms of the variables i_a , i_b , i_c , ω_r , θ_r and time as the independent variable.

3.5 SIMULATION OF BLDC MOTOR DRIVE SYSTEM

The simulation models have been developed in MATLAB environment along with SIMULINK, The SIMPOWERSYSTEM blockset has been extensively used for the purpose of simulation. Simulink is an interactive tool for modeling, simulating, and analyzing dynamic, multidomain systems. The MATLAB provides extensive tools for testing and debugging the desired system before going for final hardware implementation. This section of the chapter describes the model of

BLDC MOTOR drive system developed in MATLAB environment. All the models are developed in discrete time domain and sampling time $T = 1\mu s$.

3.5.1 Speed Controller

The model of speed controller has been realized using the simulink toolbox of the MATLAB software. The main function of speed controller block is to provide a reference torque which in turn is converted to reference current and is fed to reference generator. The output of the speed controller is limited to a proper value in accordance to the motor rating to generate the reference torque. The speed controller realized using the simulink toolbox are namely, proportional integral (PI) speed controller, fuzzy logic speed controller, hybrid speed controller and fuzzy pre-compensated proportional integral (FPPI) speed controller.

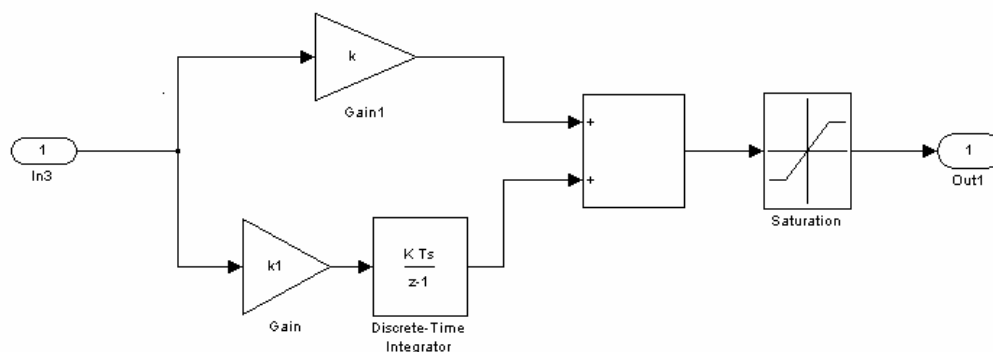


Fig 3.7 Discrete PI controller

Fig 3.7 shows the simulink model diagram of the PI controller in discrete time domain. The saturation box functions as limiter. The integral block is based upon forward Euler technique.

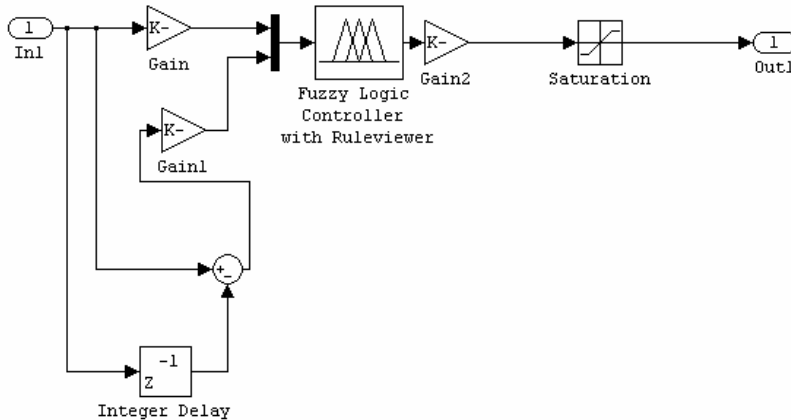


Fig 3.8 Matlab model of Fuzzy logic controller

Fig 3.8 shows the fuzzy logic speed controller in discrete time domain. The two inputs namely, speed error and change in speed error are properly scaled and fed to the MATLAB fuzzy logic controller. The defuzzified output of the fuzzy logic block after limiting forms the reference torque output. Fig 3.9 shows a hybrid controller in discrete time domain. The hybrid speed controller combines the output from fuzzy logic controller and PI controller. The contribution pattern has already been discussed in the previous section. The PI weight block and fuzzy

logic weight block determines the contribution factor depending upon the operating region. The final output is the combination of the both controller output. Fig 3.10 shows the FPPI speed controller in discrete time domain. The FL controller provides the modified reference speed signal, from which the speed error is calculated and is fed to the PI controller as the reference speed signal.

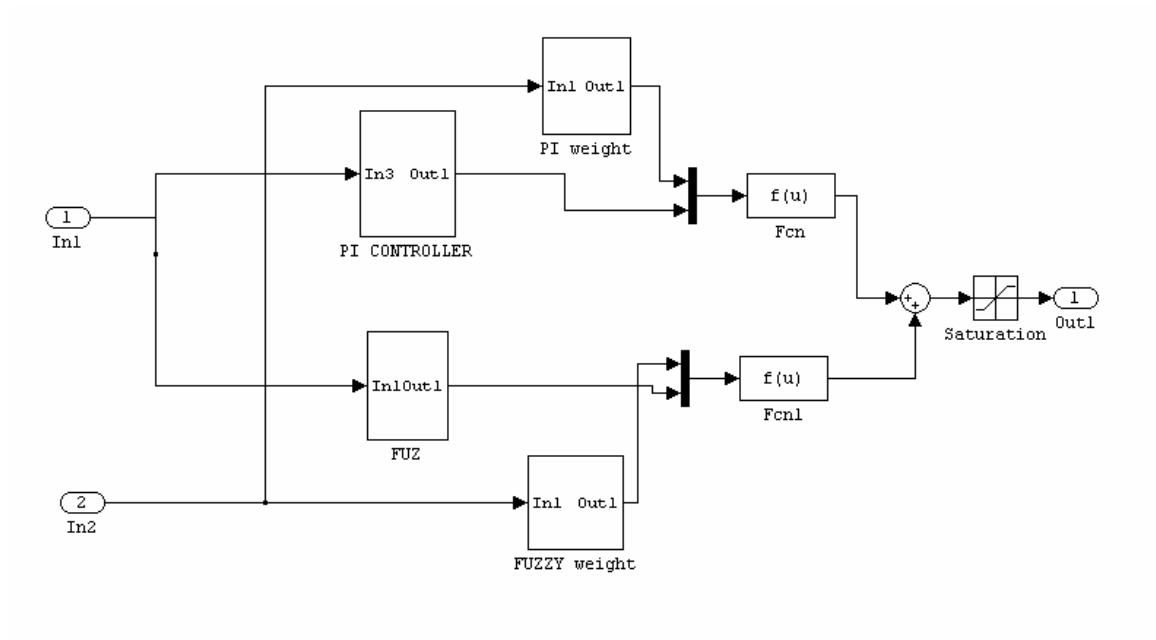


Fig 3.9 Matlab model of Hybrid controller

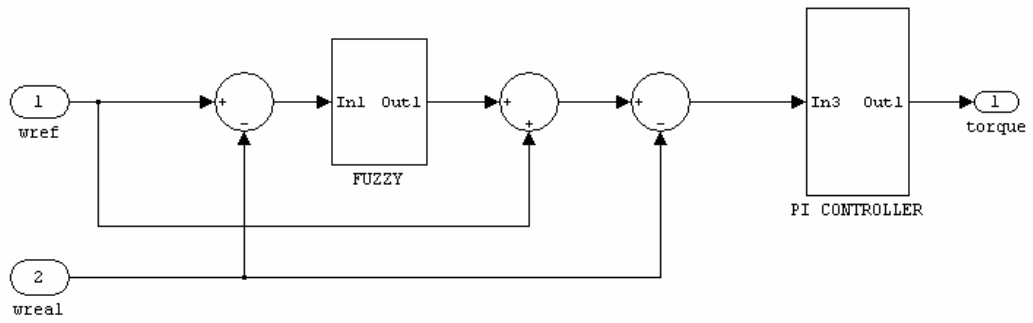


Fig 3.10 Matlab model of fuzzy pre-compensated model

3.5.2 Reference Generator

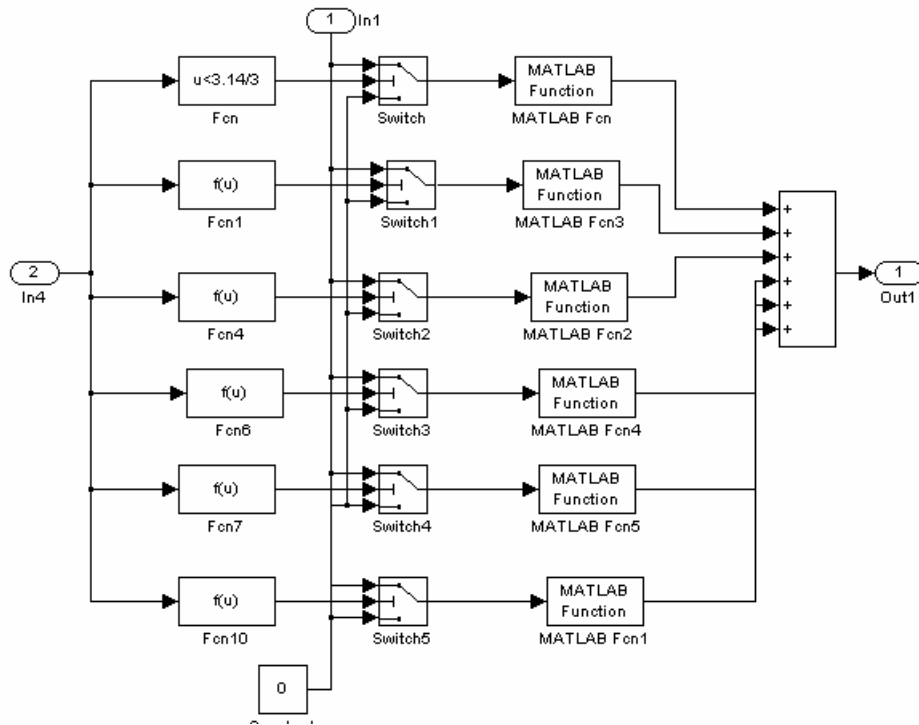


Fig 3.11 Matlab model of Reference generator

Fig 3.11 shows the MATLAB model of reference generation block. The functioning of the block has already been discussed in the previous section. The input to the block is the reference current and output is a vector consisting of reference current signal for each phase. The components of the vector form the reference signal for each of the three phases.

3.5.3 Hysteresis Controller And Inverter

Fid 3.12 shows the Hysteresis controller along with the inverter. The input is the reference current and the actual current following in the motor. The output is modulated voltage which is being fed to the motor.

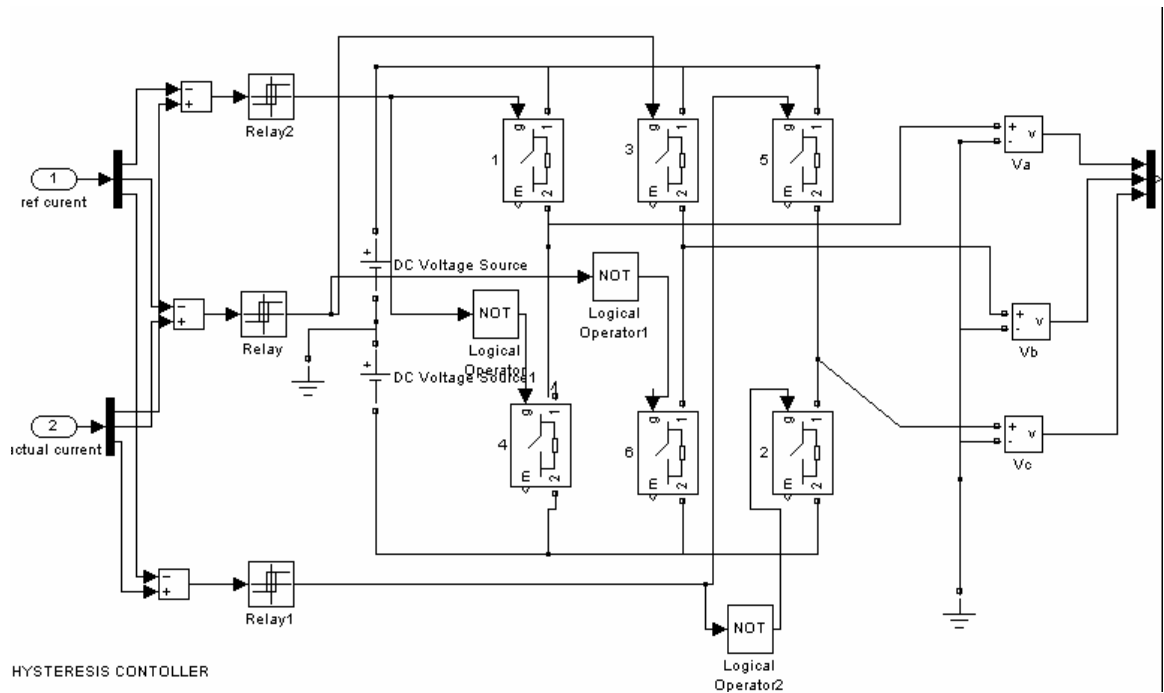


Fig 3.12 Matlab model of Hysteresis controller with inverter

3.5.4 Position Detection Unit

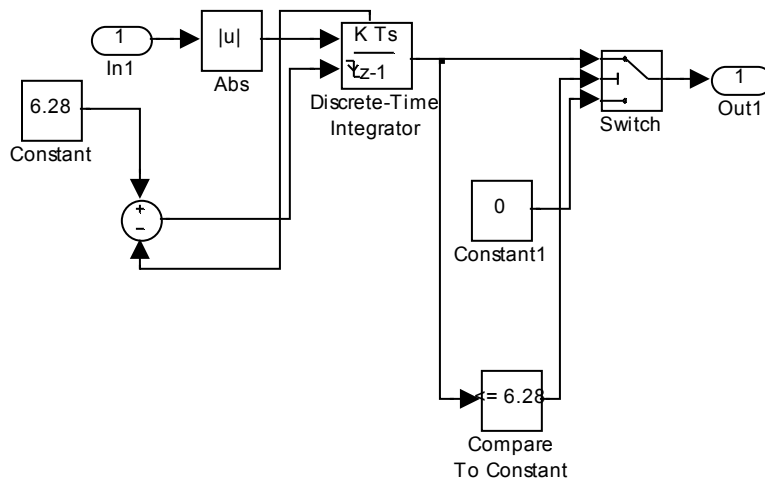


Fig 3.13 Matlab model of position detection block

Fig 3.13 shows the position detection block. The input to the block is angular velocity and output is angular displacement of the rotor. The integrator has been approximated by forward Euler method.

3.5.5 Brushless DC Motor

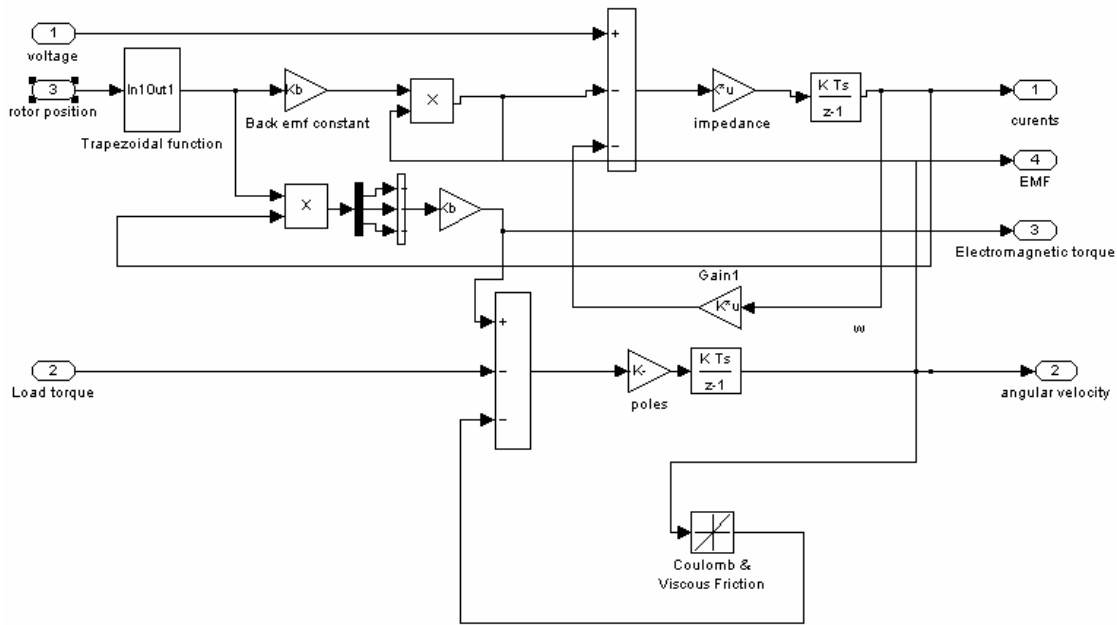


Fig 3.14 Matlab model of BLDC MOTOR motor

Fig 3.14 shows the Brushless DC motor in discrete time domain. The inputs to the block are the modulated voltage, position of the rotor, and the load torque. The outputs are angular velocity, electromagnetic voltage, phase currents and the produced torque. The lower part of the model is based upon the mechanical equation (16) of the motor. The input to this part is load torque. The upper part of the model is based upon the electrical equation (19) of the motor. The inputs to this part are rotor position and voltage.

3.5.6 Complete System

Fig 3.15 shows the complete setup of the BLDC MOTOR motor drive. The input to the system is reference speed. The scope provides the snapshot of the output quantities.

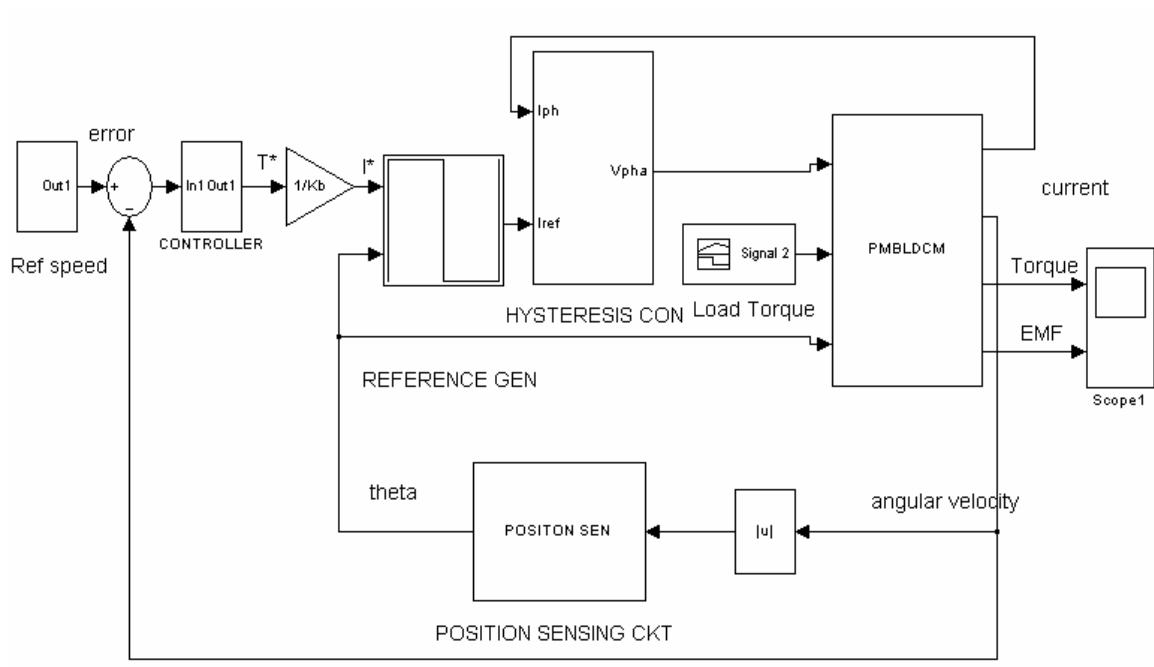


Fig 3.15 Matlab model of complete BLDC MOTOR drive system

3.6 RESULTS AND DISCUSSIONS

The performance of the BLDC MOTOR drive system is simulated using developed mathematical model in MATLAB environment along with simulink and simpower system blockset under different dynamic conditions such as starting, speed reversal and load perturbation (load application and load removal). A set of response comprises of reference speed (ω_r^*), rotor speed (ω_r) in electrical rad/sec, three phase winding currents in Amperes, developed electromagnetic

torque and load torque in Nm. The discrete system has been executed at sampling interval of $1\mu\text{s}$.

The performance for starting, speed reversal and load perturbation is shown in Fig 3.16-3.59 corresponding to 2 hp brushless DC motor drive. The controller parameters and motor parameters are given in the Appendix-I. From the obtained results the following salient features are observed.

3.6.1 Starting Dynamics

The reference speed is set at 140 rad/s with a torque limit equal to the rated torque produced by the motor. Initially, the motor accelerates with maximum torque to reach the reference speed as soon as possible. When the speed error reduces to the almost zero rad/s, the winding current also decreases to that of no-load value and the developed torque becomes equal to no-load value.

3.6.2 Reversal Dynamics

The speed reversal dynamics are also shown in the Figs 3.16-3.59. While the motor is running at steady speed of 140 rad/s, the reference speed is changed to -140 rad/s. In response to this change, the controller changes the direction of the flow of current in the windings to negative direction which results in the regenerative braking of the motor. Since just before and after the reversal phenomenon the drive is in the same dynamic state(no load condition), the steady state values of the current are observed to same in magnitude.

3.6.3 Load Perturbation

As shown in the Figs 3.16-3.59, when the motor is running at a steady state of 140 rad/s,, a load torque equal to the rated torque is applied to the motor shaft.

Sudden application of the load torque results in the fall of the speed of the motor. In response to the drop in speed, the output of the speed controller responds by increasing the reference torque value. Therefore, the developed electromagnetic torque of the BLDC MOTOR motor increases causing the motor speed to settle to the reference value with the increased winding currents.

3.6.4 Response of Drive using Different Controllers

1. PI Controller

a) Under load perturbation

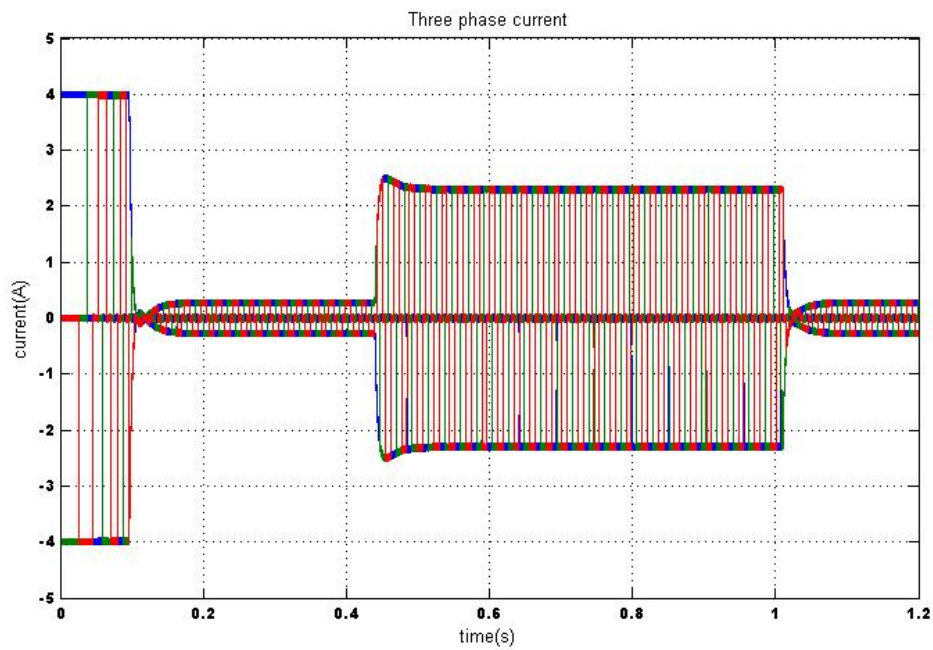


Fig 3.16 Three phase current under load perturbation for PI controller

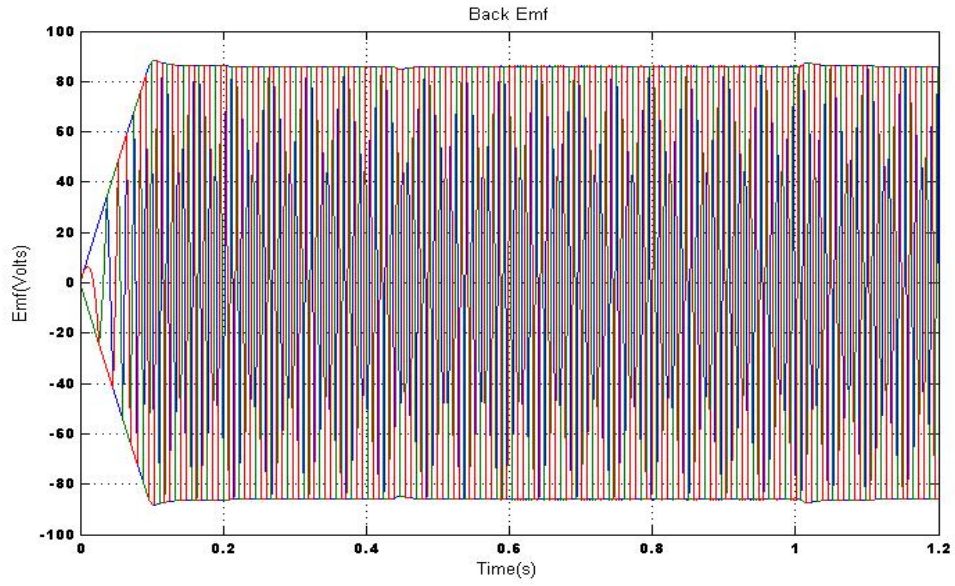


Fig 3.17 Back Emf produced under load perturbation for PI controller

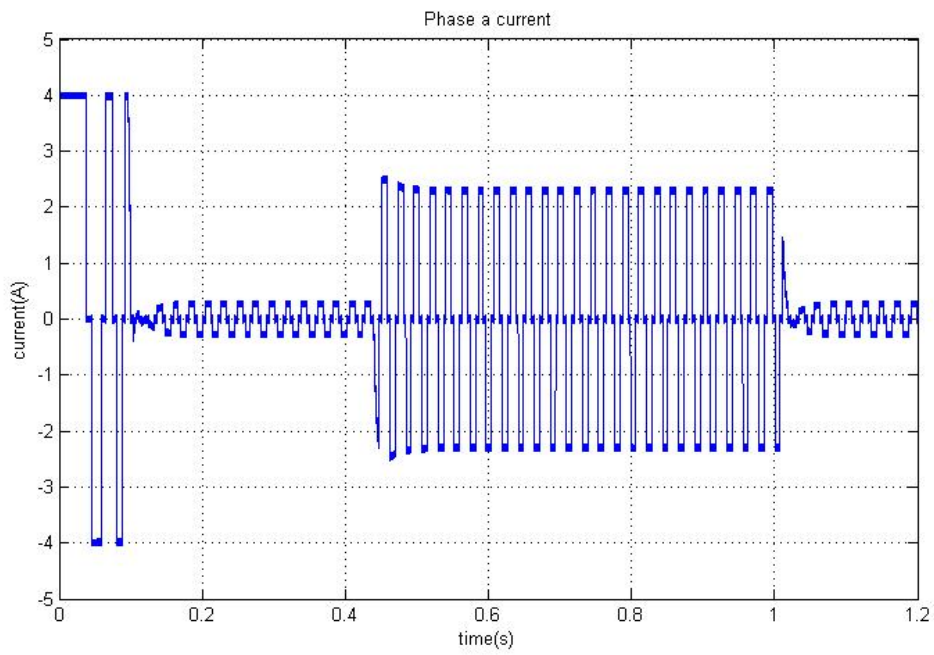


Fig 3.18 Phase 'a' current under load perturbation for PI controller

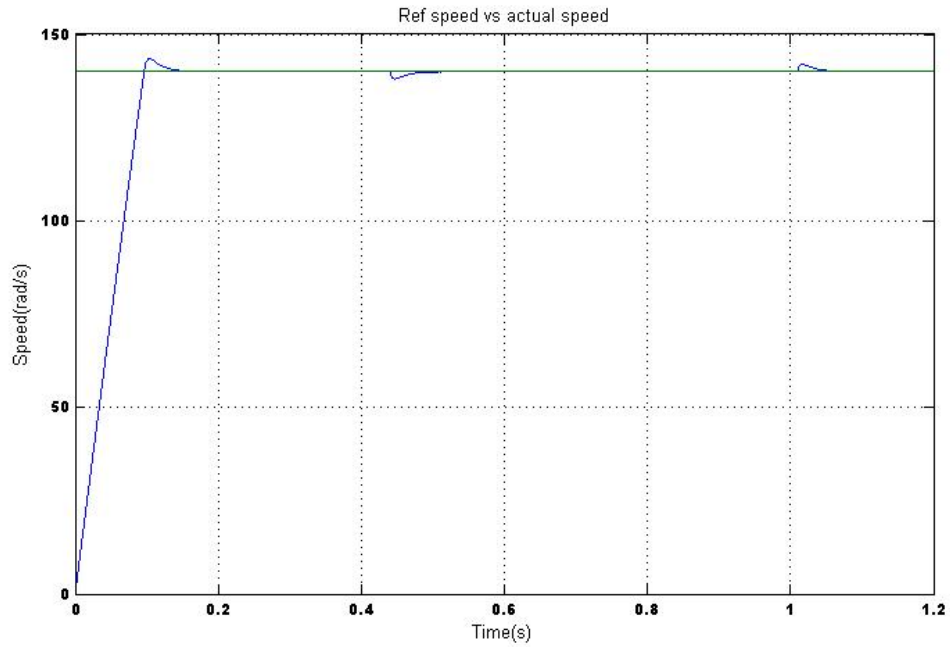


Fig 3.19 Reference speed Vs real speed response under load perturbation for PI controller

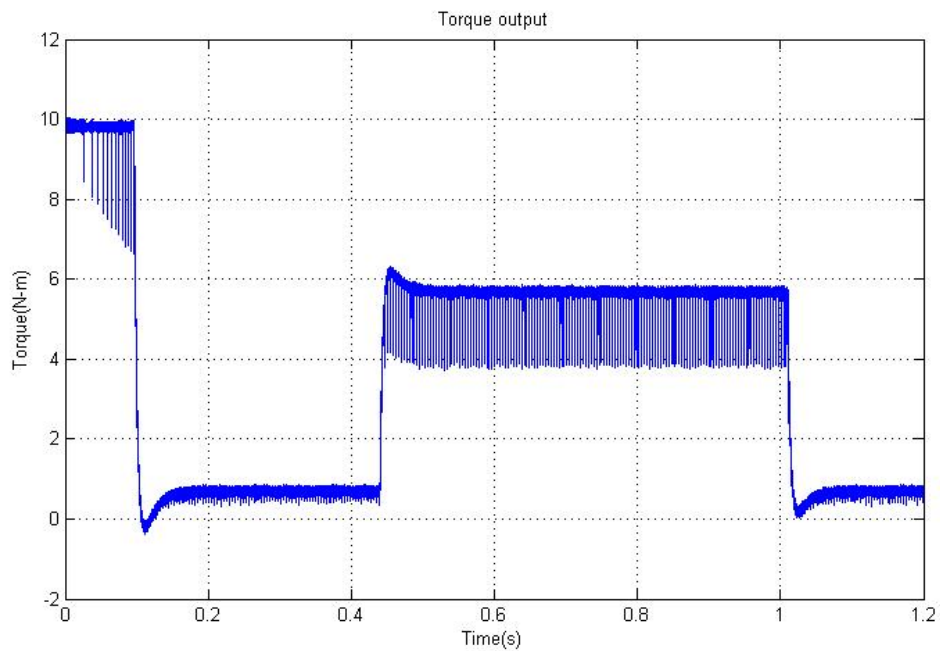


Fig 3.20 Electromagnetic Torque produced under load perturbation for PI controller

b) Under Speed Reversal

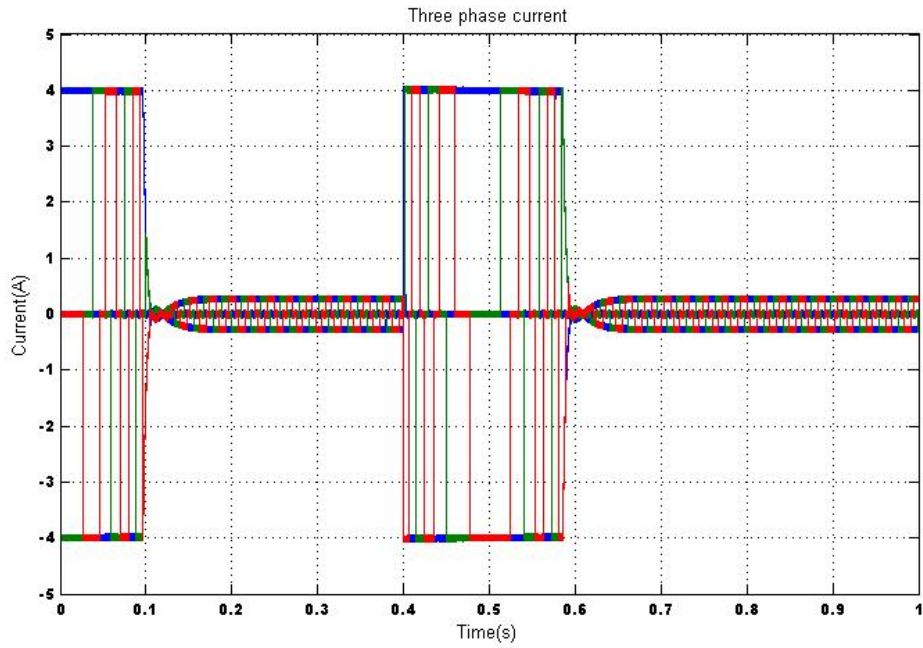


Fig3.21 Three phase current under speed reversal for PI controller

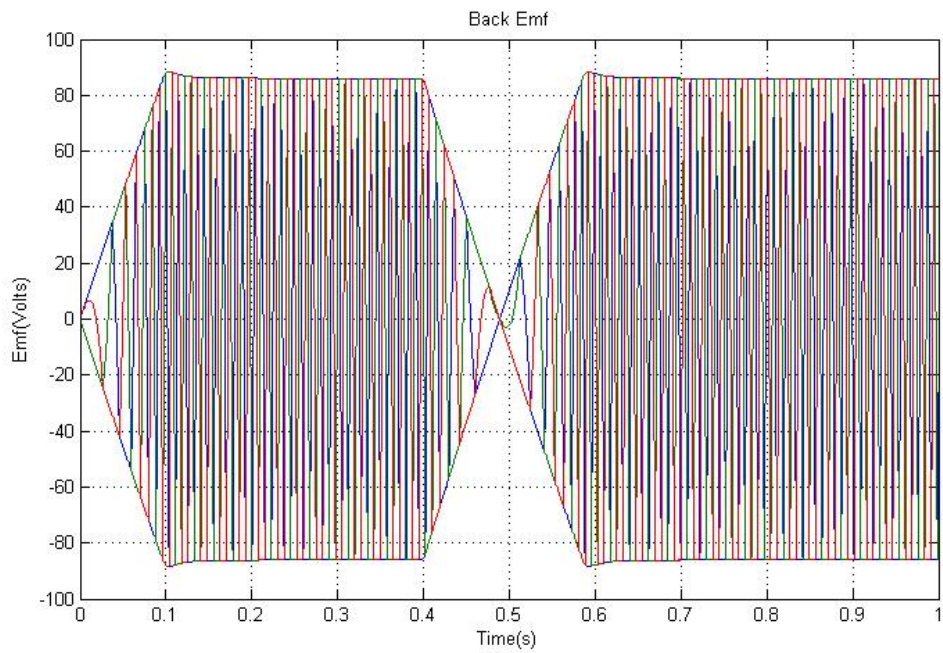


Fig 3.22 Back Emf produced under speed reversal for PI controller

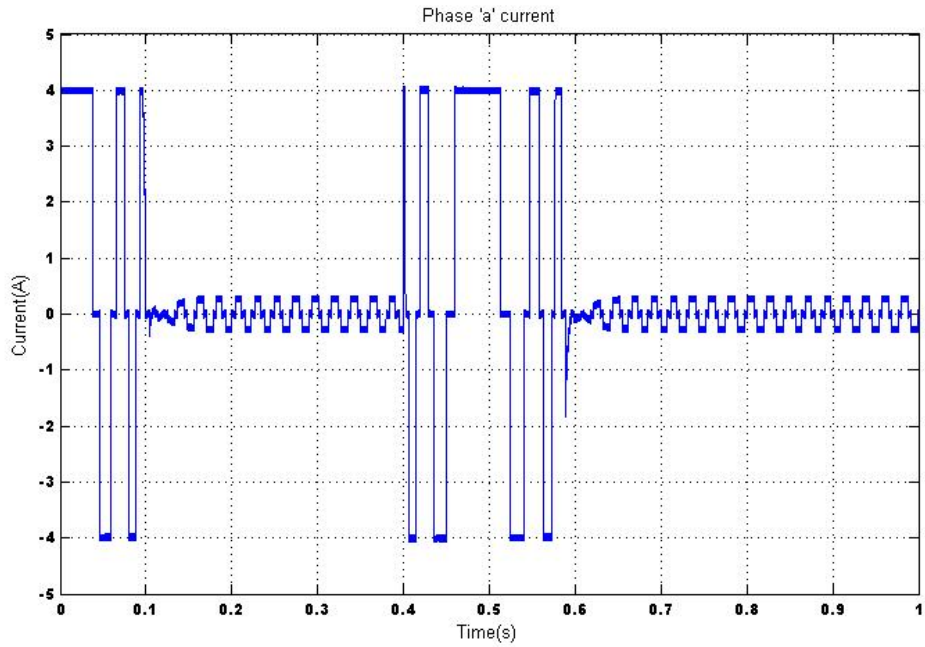


Fig 3.23 Phase 'a' current under speed reversal for PI controller.

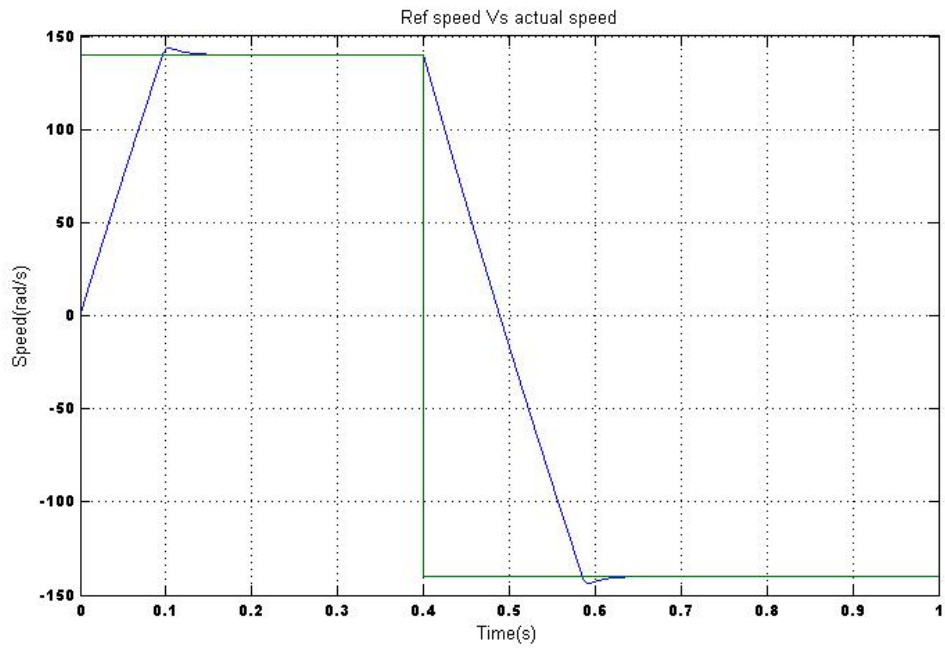


Fig 3.24 Reference speed Vs real speed response under speed reversal for PI controller

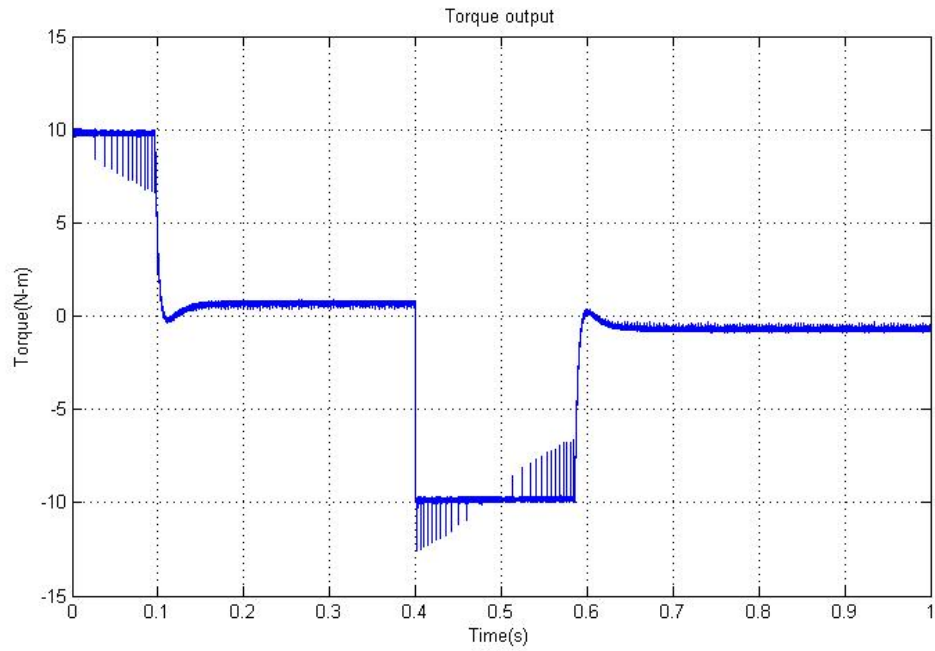


Fig 3.25 Electromagnetic Torque produced under speed reversal for PI controller

2. Fuzzy Controller

a) Under load perturbation

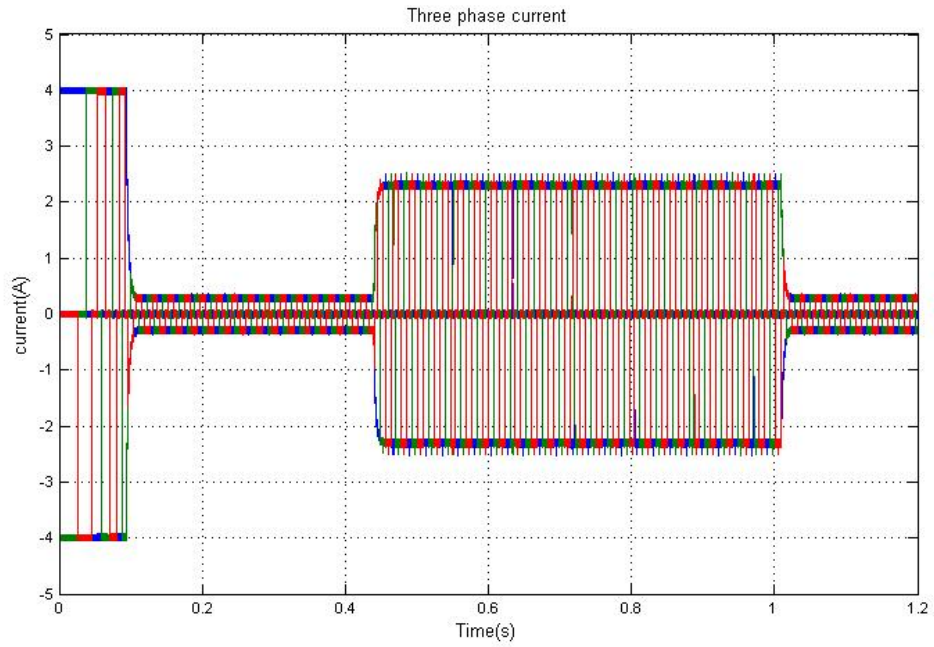


Fig 3.26 Three phase current under load perturbation for Fuzzy controller.

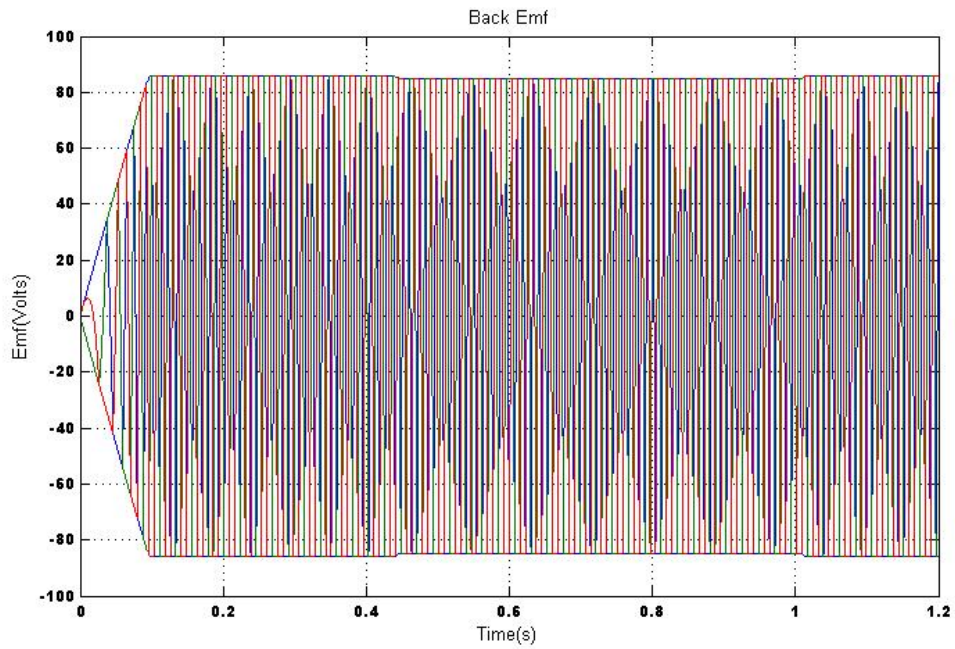


Fig 3.27 Back Emf produced under load perturbation for Fuzzy controller.

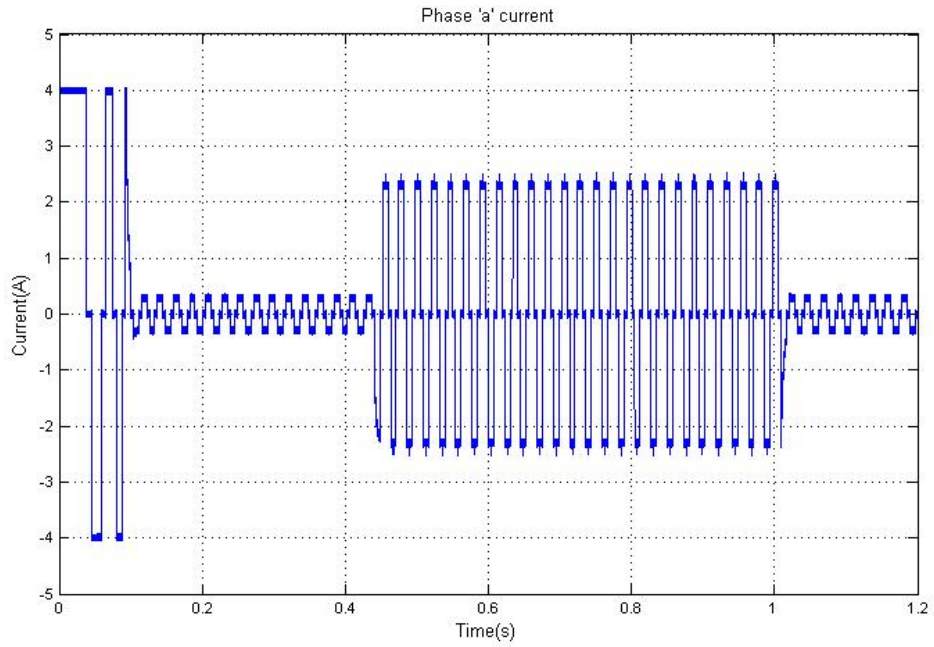


Fig 3.28 Phase 'a' current under load perturbation for Fuzzy controller

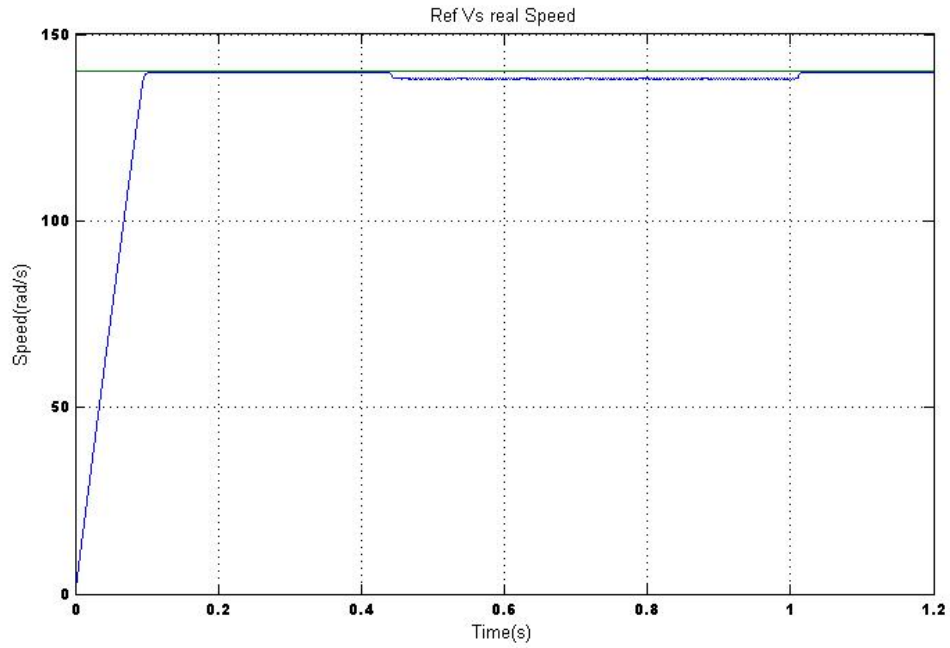


Fig 3.29 Reference speed Vs real speed response under load perturbation for Fuzzy controller

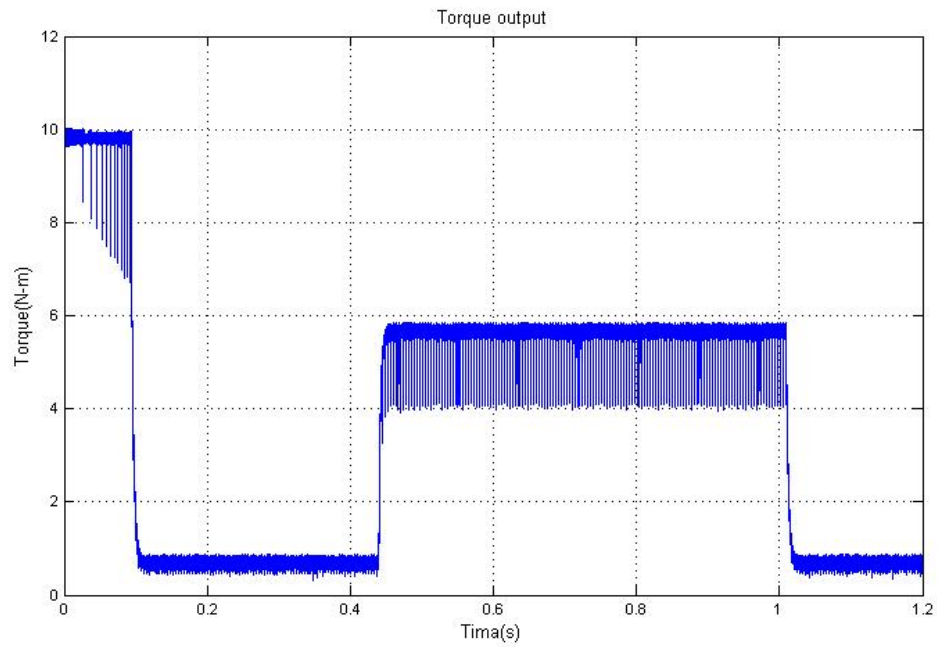


Fig 3.30 Electromagnetic Torque produced under load perturbation for Fuzzy controller

b) Under speed reversal

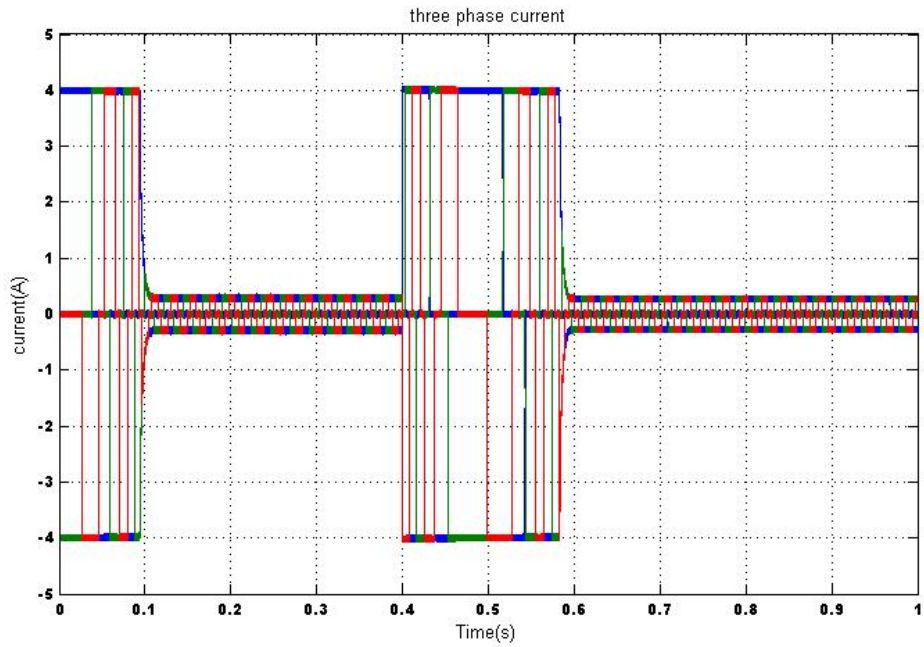


Fig 3.31 Three phase current under speed reversal for Fuzzy controller

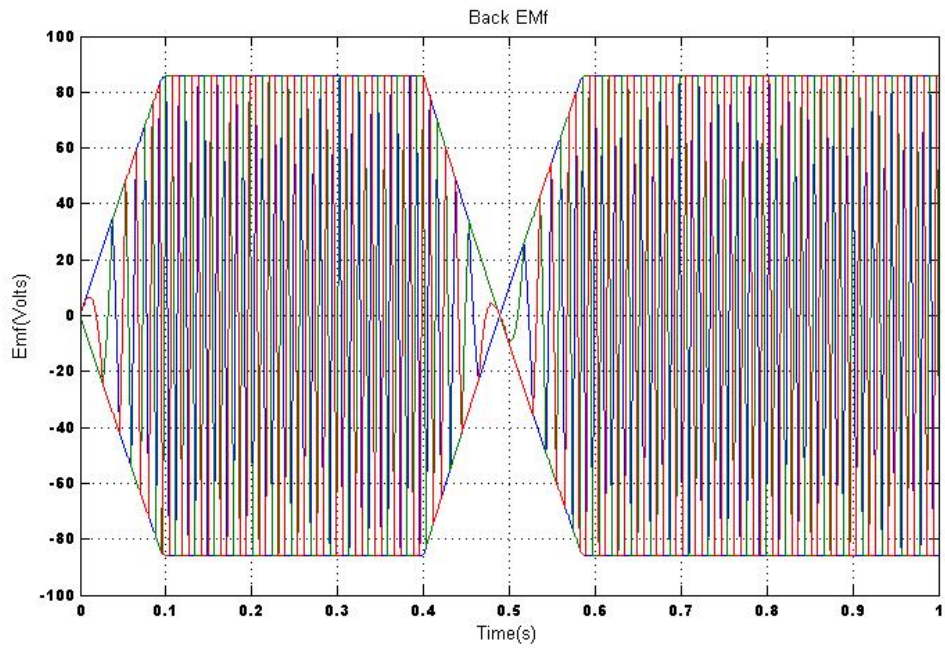


Fig 3.32 Back Emf produced under speed reversal for Fuzzy controller

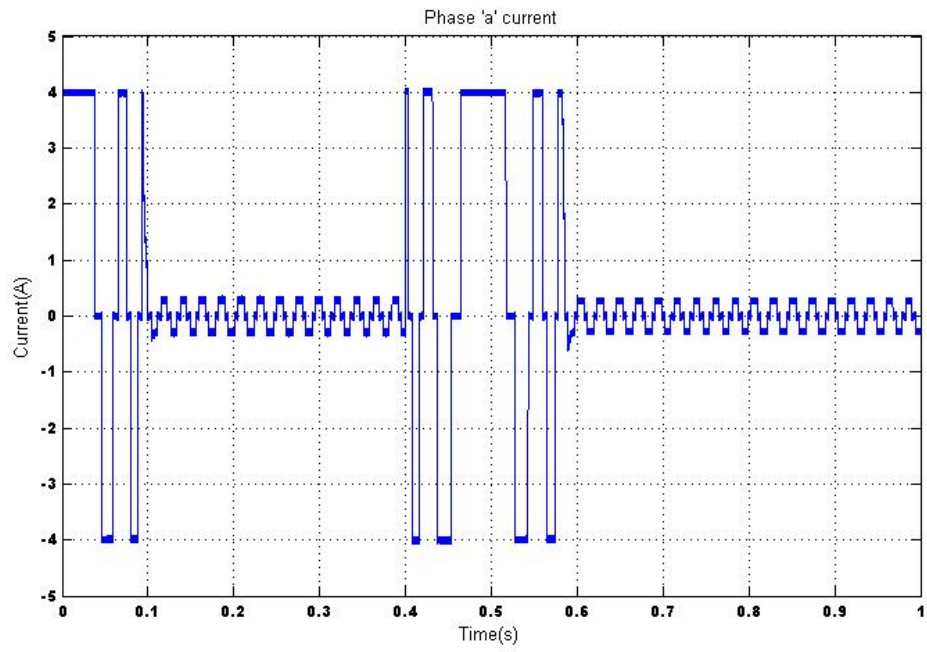


Fig 3.33 Phase 'a' current under speed reversal for Fuzzy controller.

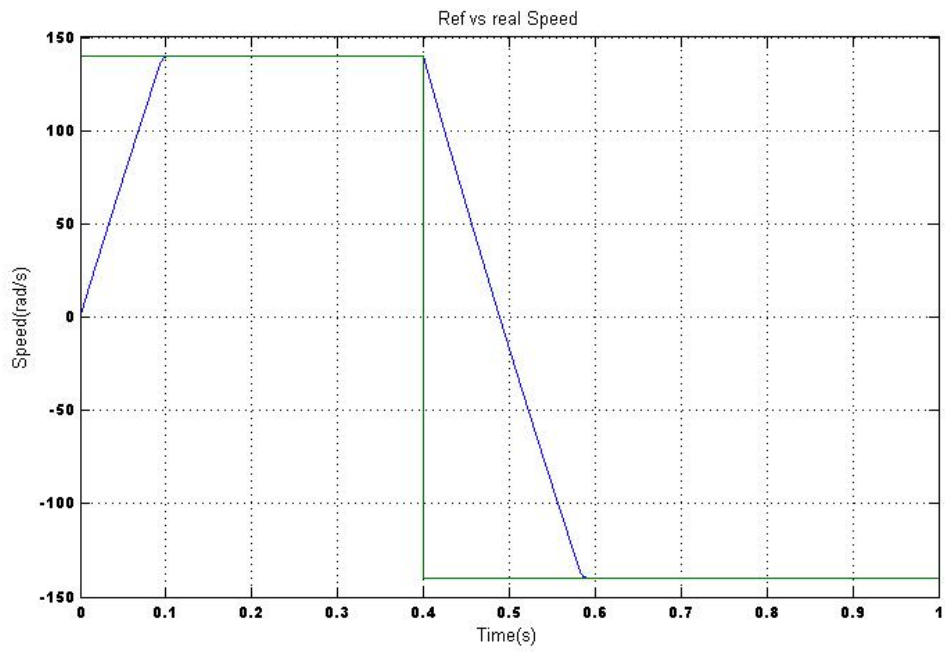


Fig 3.34 Reference speed Vs real speed response under sped reversal for Fuzzy controller

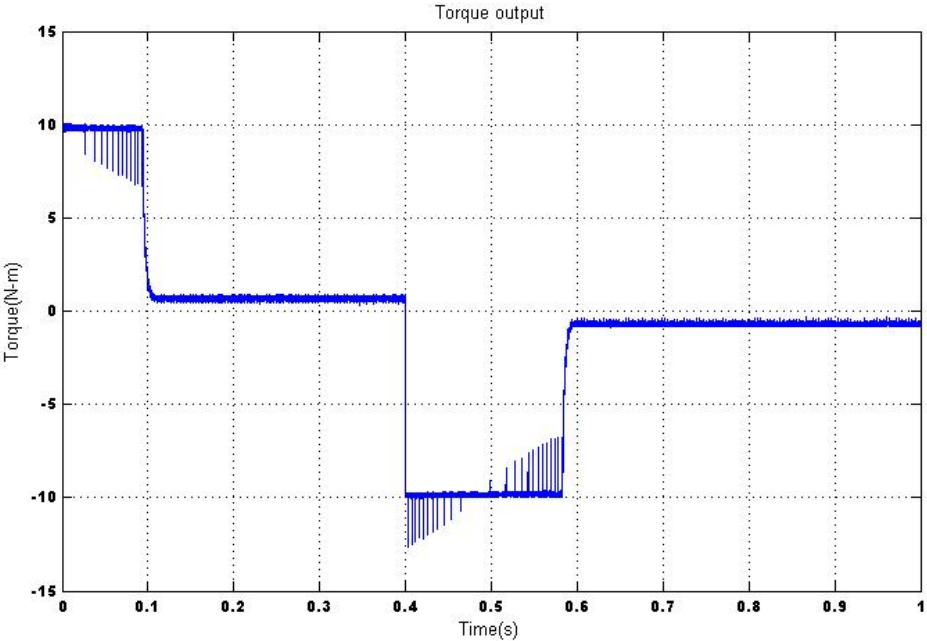


Fig 3.35 Electromagnetic Torque produced under speed reversal for Fuzzy controller

3. Hybrid Controller

a) Under load perturbation

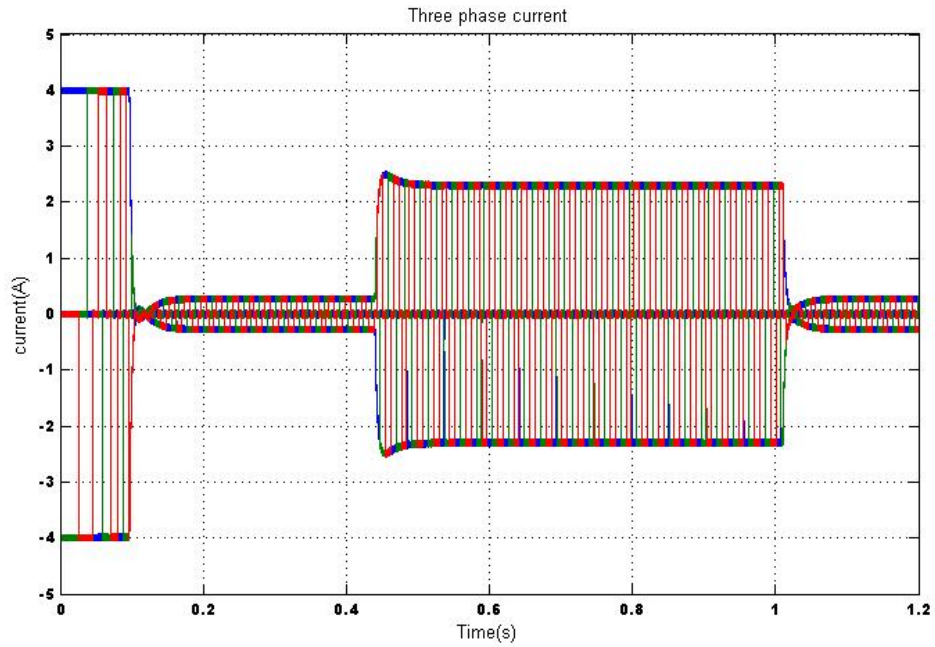


Fig 3.36 Three phase current under load perturbation for Hybrid controller.

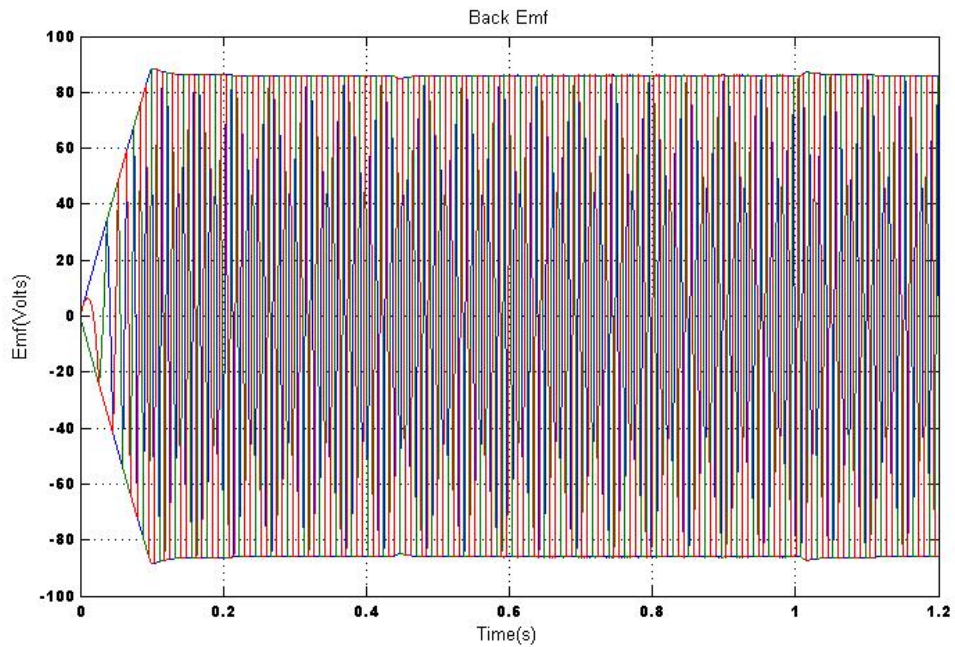


Fig 3.37 Back Emf produced under load perturbation for Hybrid controller.

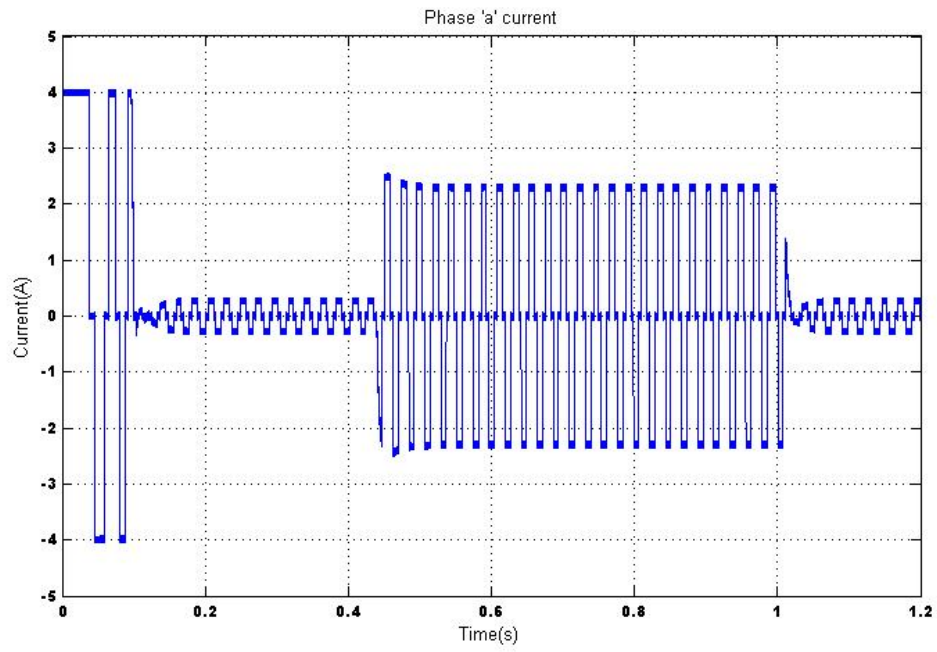


Fig 3.38 Phase 'a' current under load perturbation for Hybrid controller

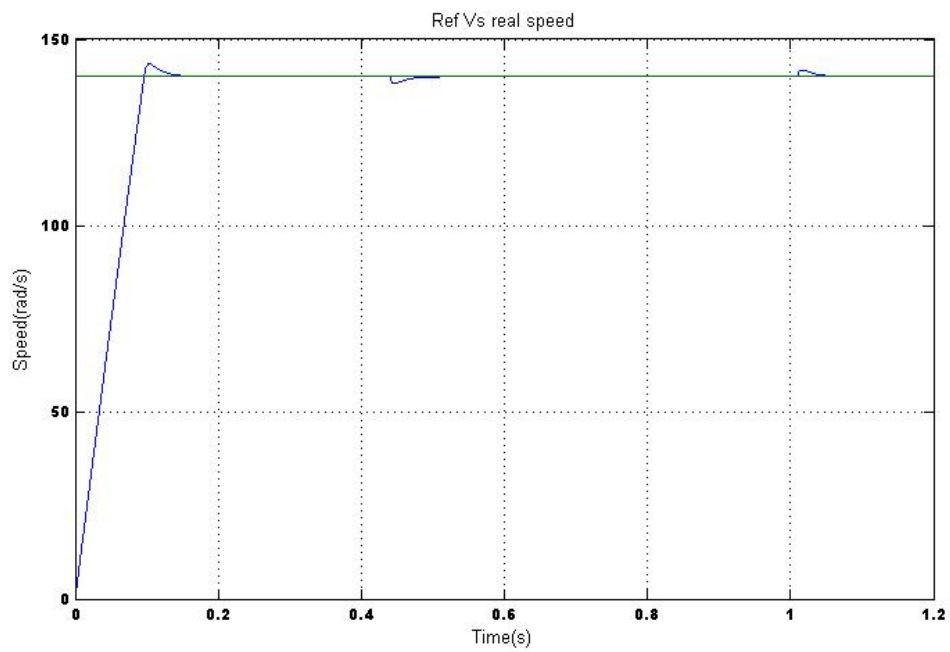


Fig 3.39 Reference speed Vs real speed response under load perturbation for Hybrid controller

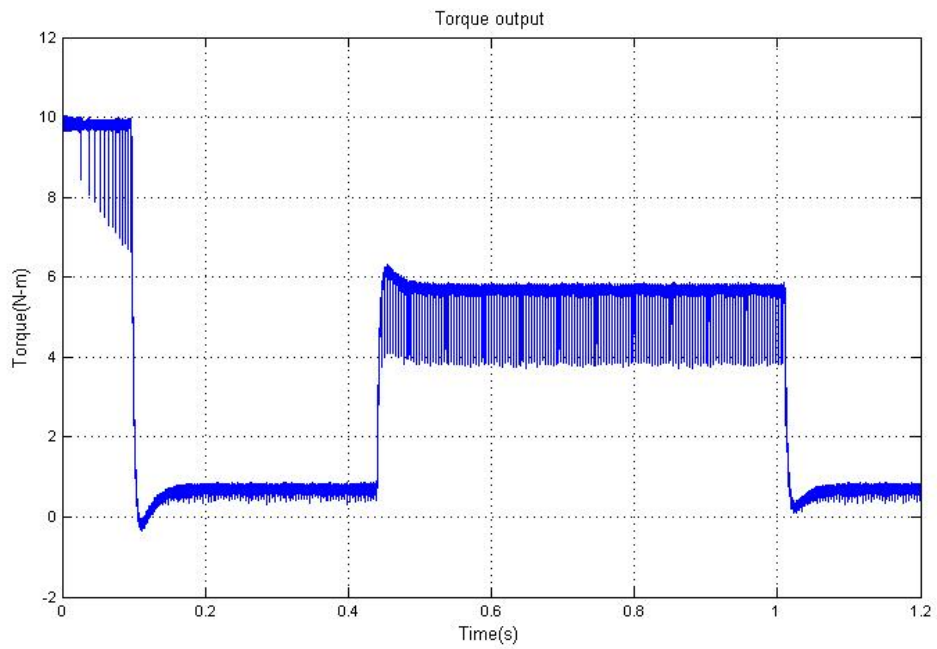


Fig 3.40 Electromagnetic Torque produced under load perturbation for Hybrid controller

b) Under speed reversal

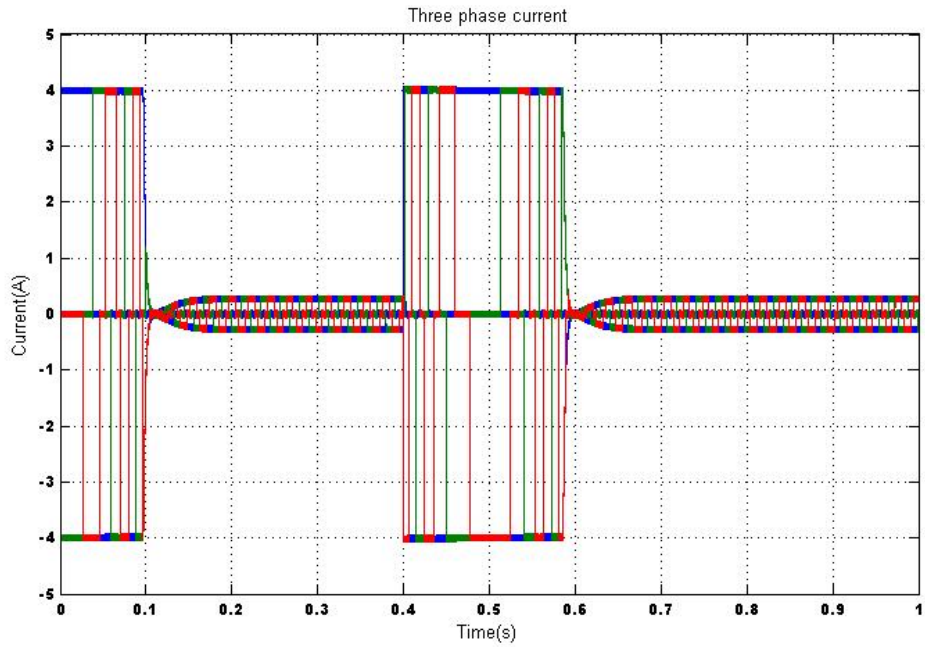


Fig 3.41 Three phase current under speed reversal for Hybrid controller.

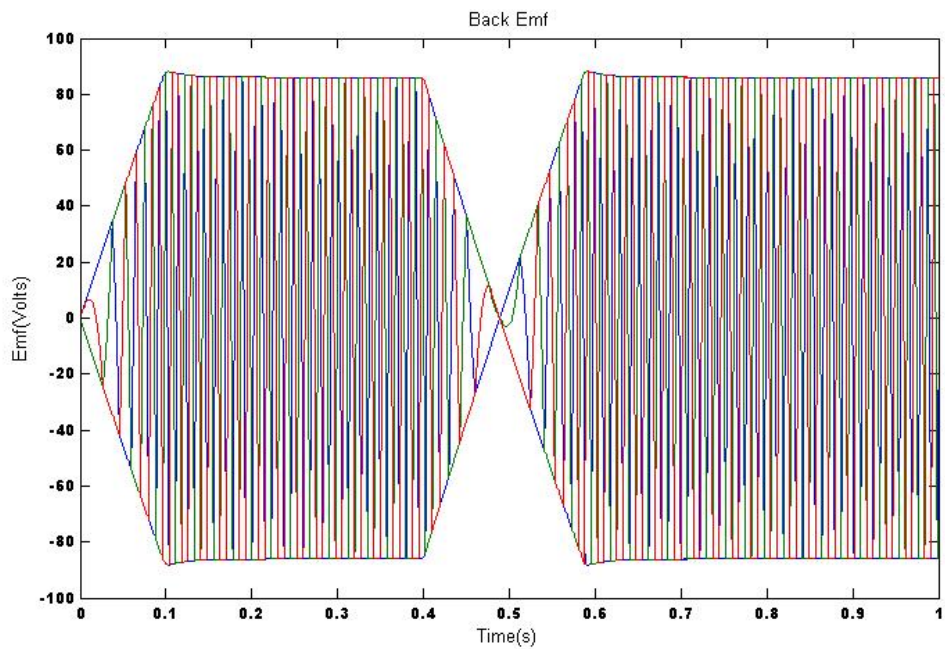


Fig 3.42 Back Emf produced under speed reversal for Hybrid controller

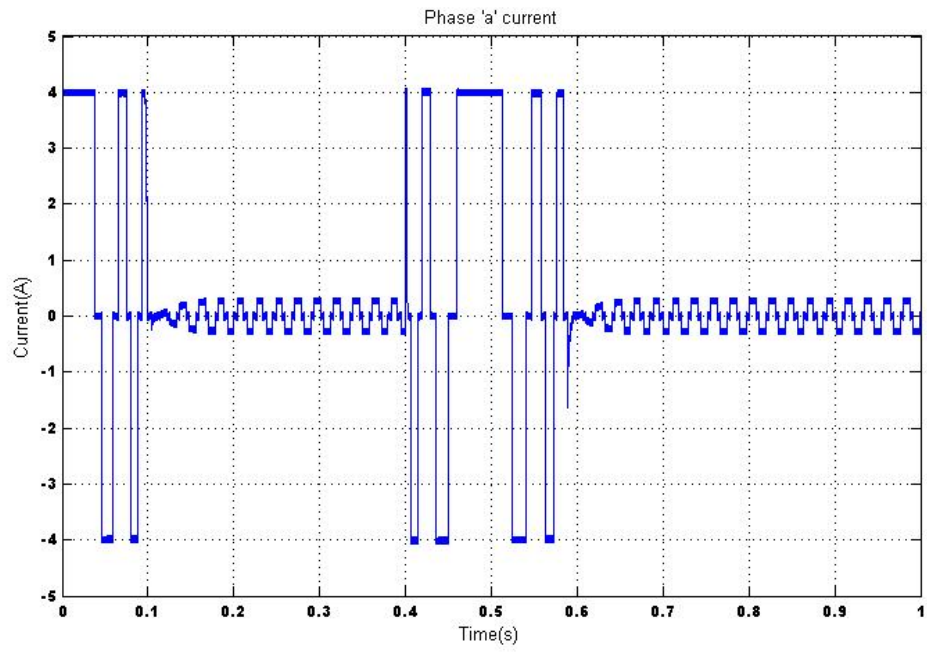


Fig 3.43 Phase 'a' current under speed reversal for Hybrid controller

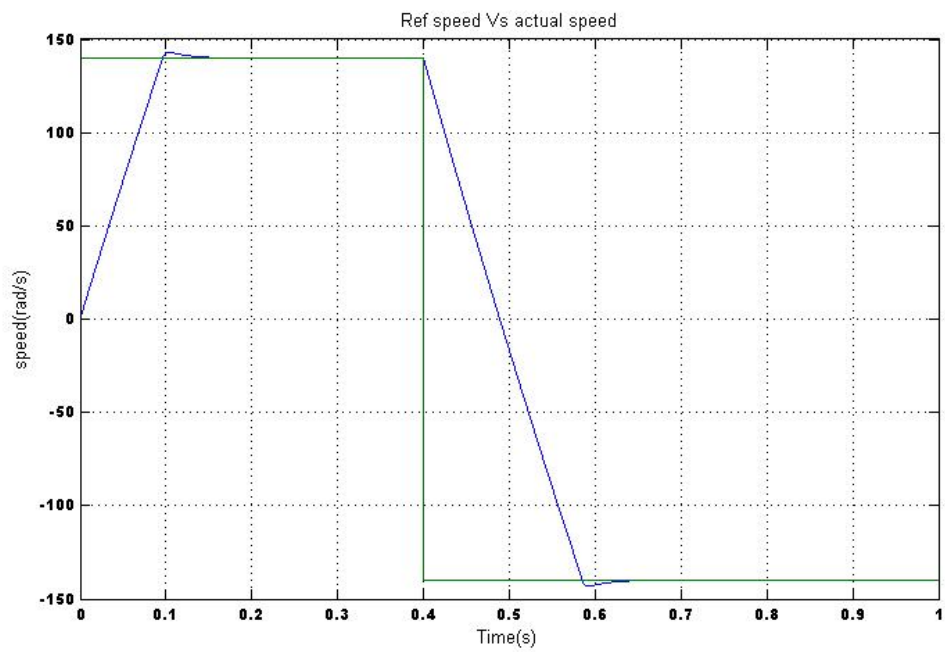


Fig 3.44 Reference speed Vs real speed response under speed reversal for Hybrid controller

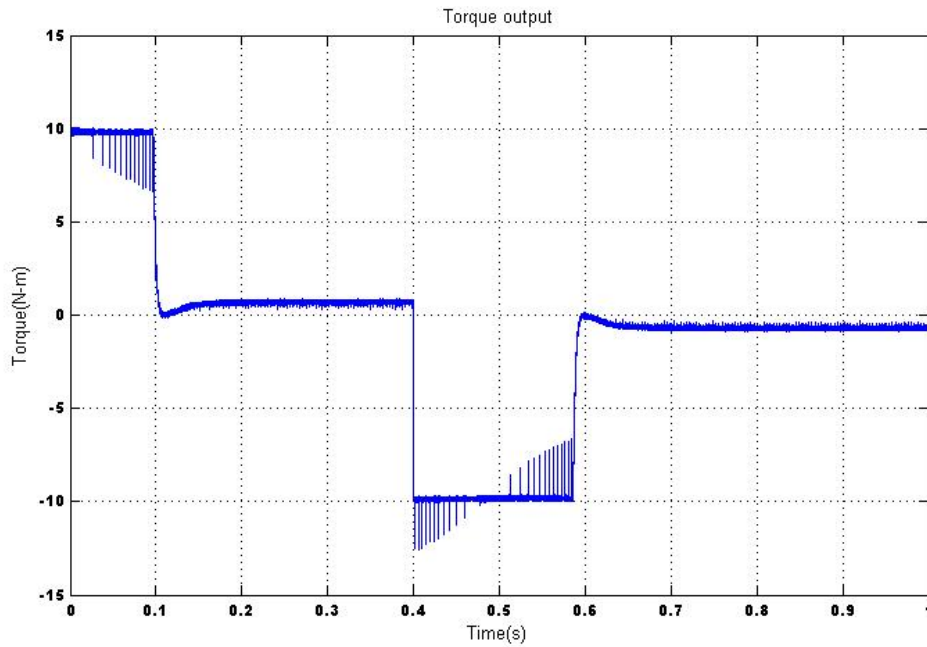


Fig 3.45 Electromagnetic Torque produced under speed reversal for Hybrid controller

4. Fuzzy Pre-compensated PI controller

a) Under load perturbation

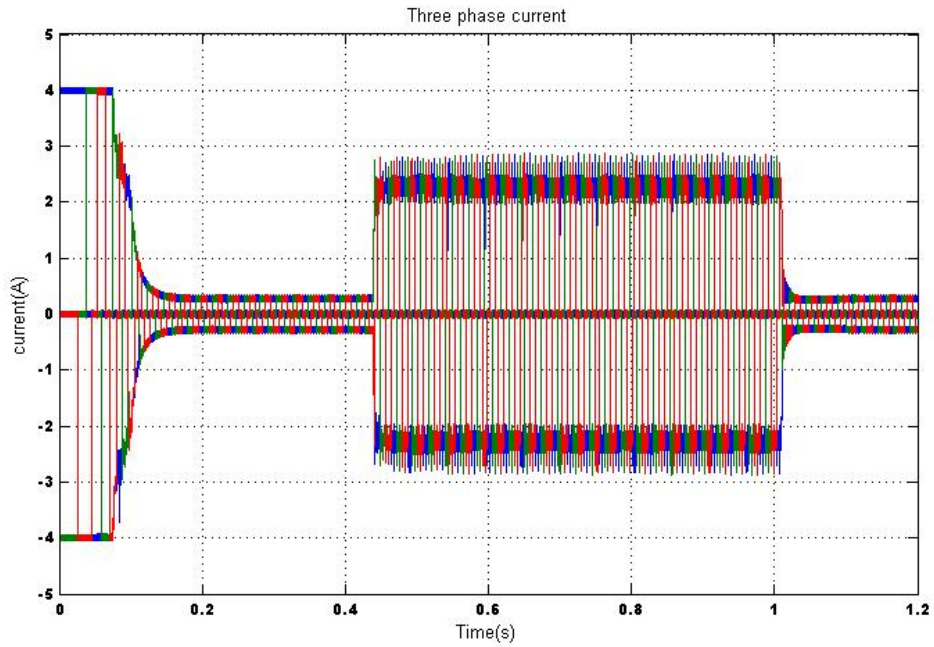


Fig 3.46 Three phase current under load perturbation for FPCPI controller.

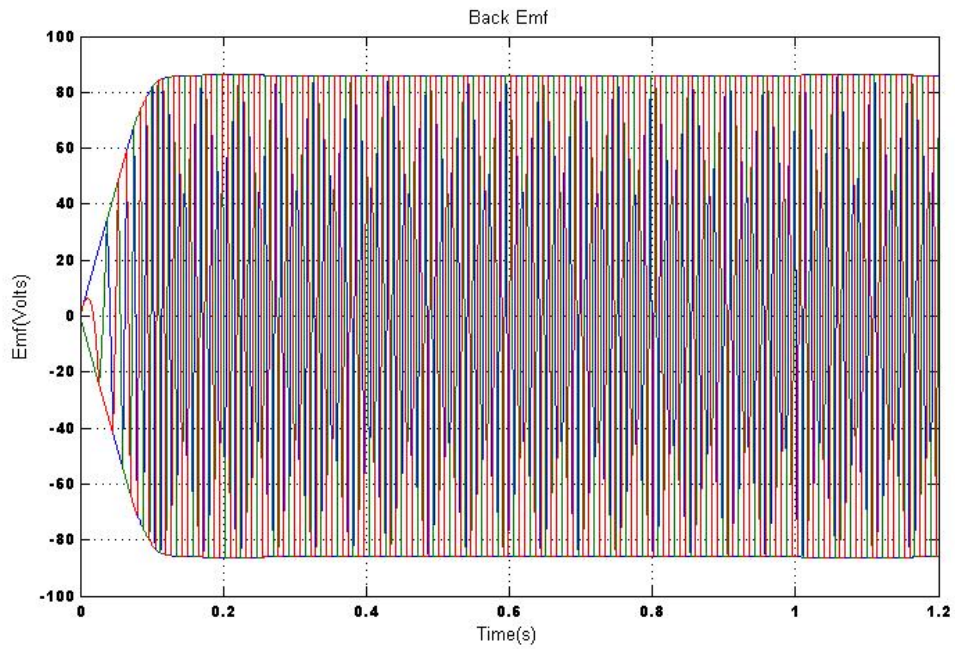


Fig 3.47 Back Emf produced under load perturbation for FPCPI controller

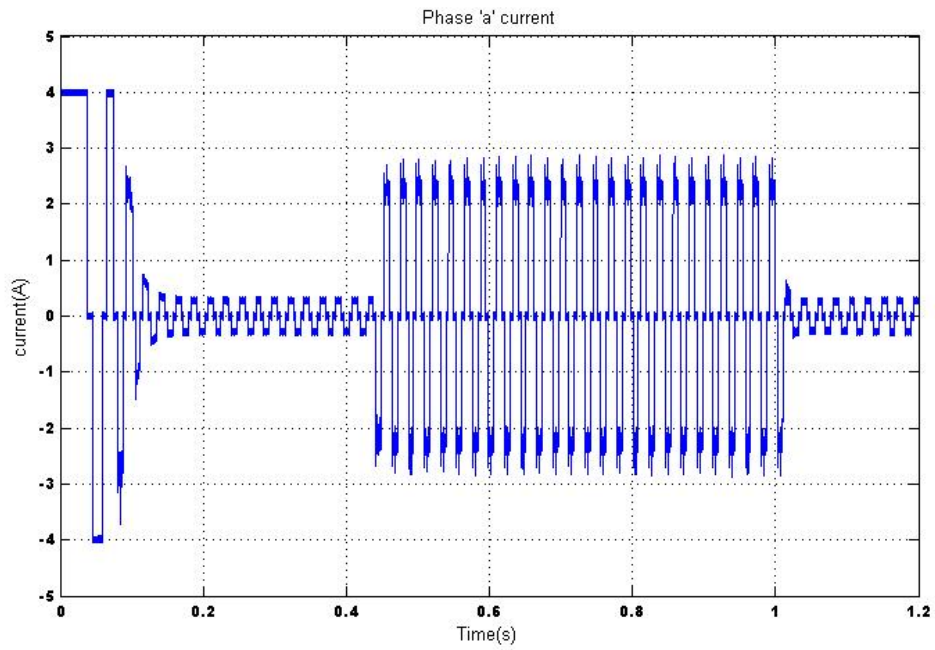


Fig 3.48 Phase 'a' current under load perturbation for FPCPI controller

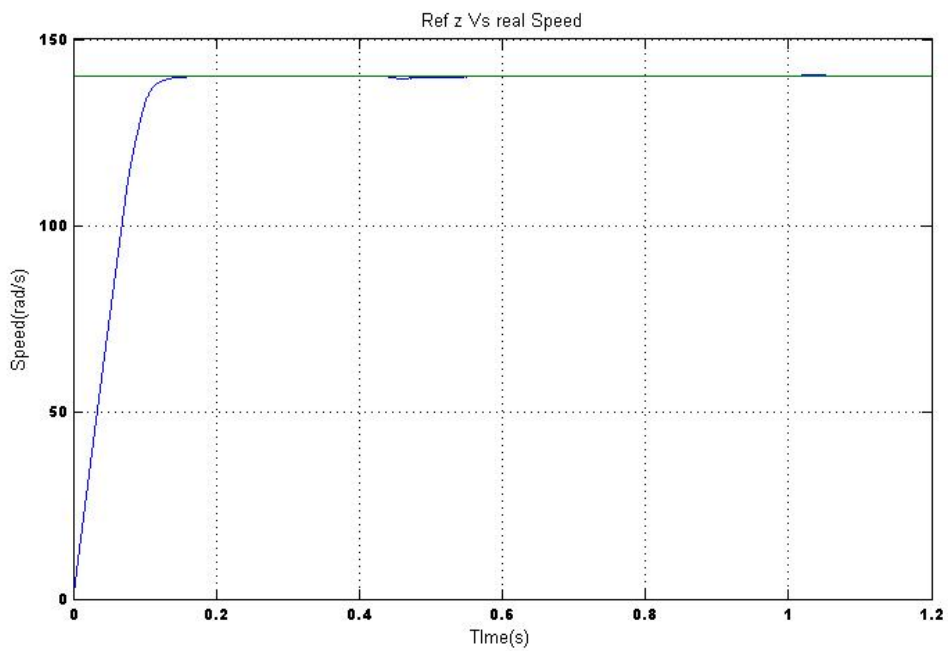


Fig 3.49 Reference speed Vs real speed response under load perturbation for FPCPI controller

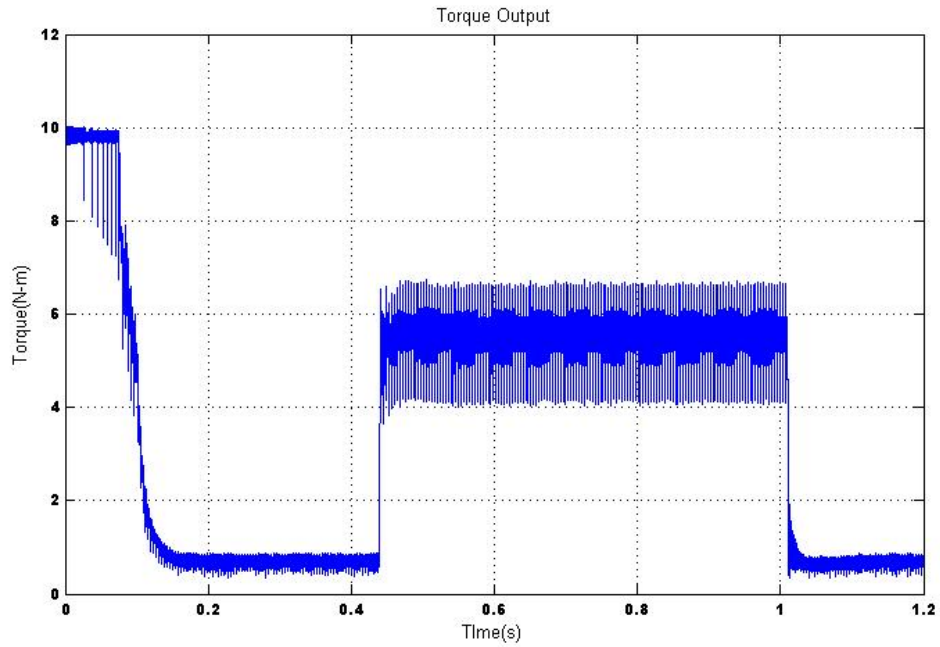


Fig 3.50 Electromagnetic Torque produced under load perturbation for FPCPI controller

b) Under speed reversal

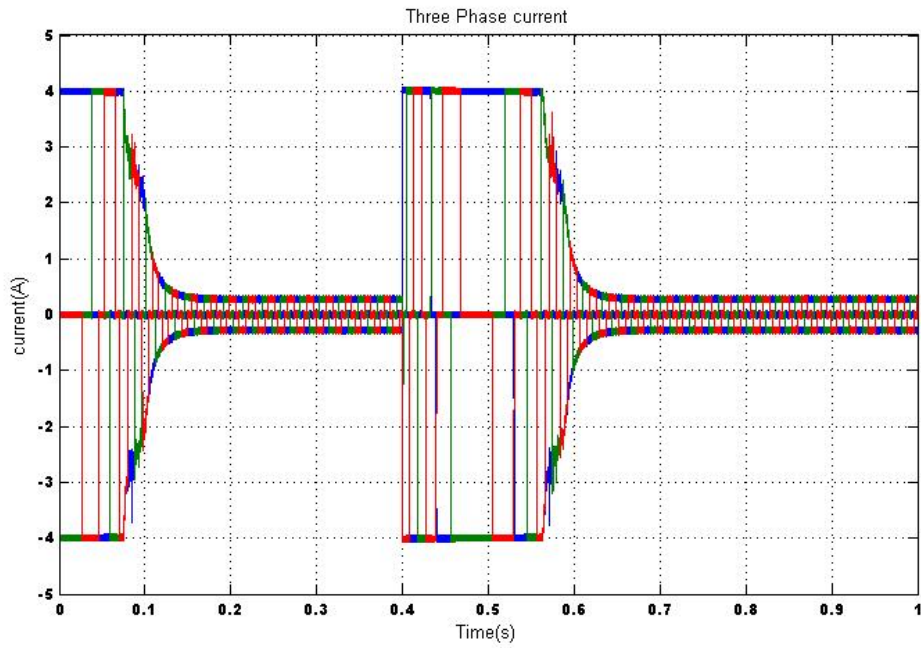


Fig 3.51 Three phase current under speed reversal for FPCPI controller

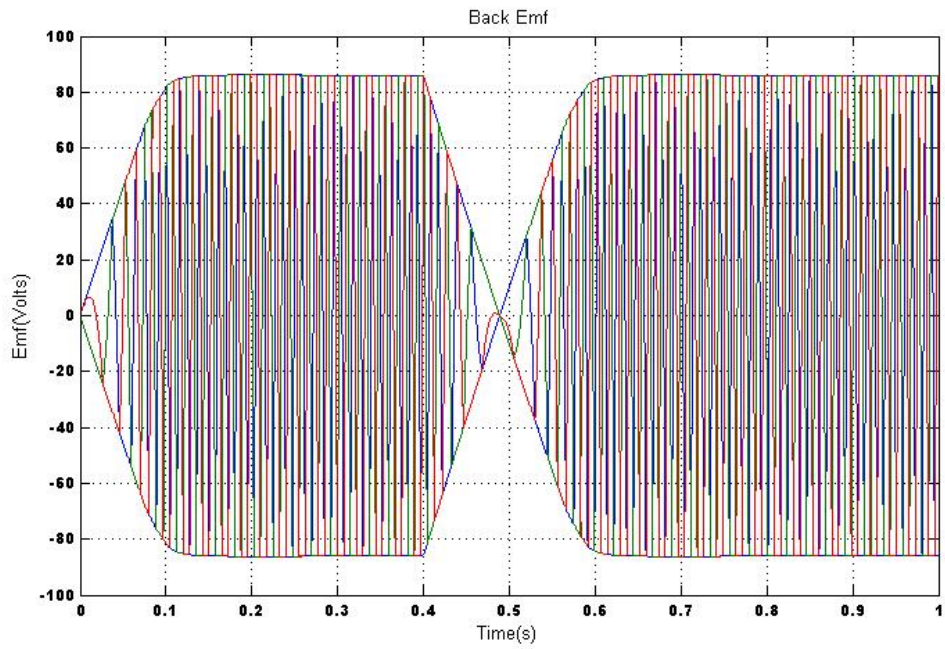


Fig 3.52 Back Emf produced under speed reversal for FPCPI controller

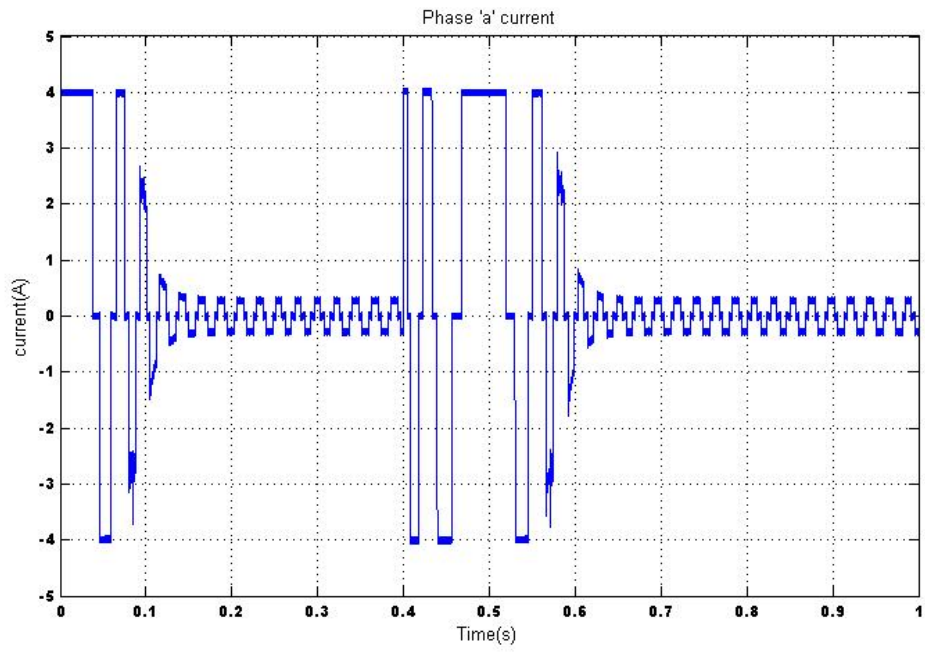


Fig 3.53 Phase 'a' current under speed reversal for FPCPI controller

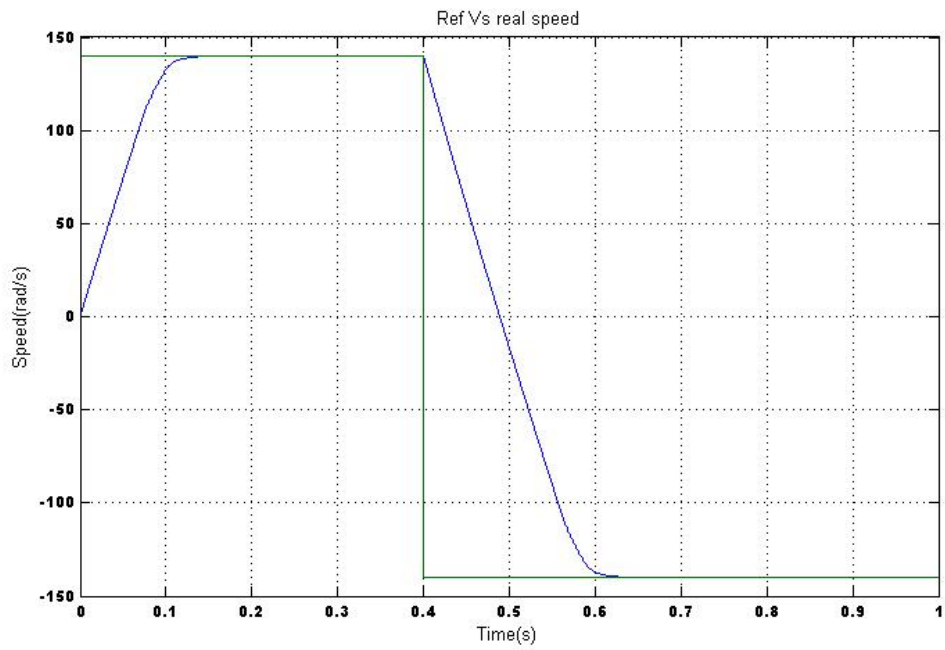


Fig 3.54 Reference speed Vs real speed response under speed reversal for FPCPI controller

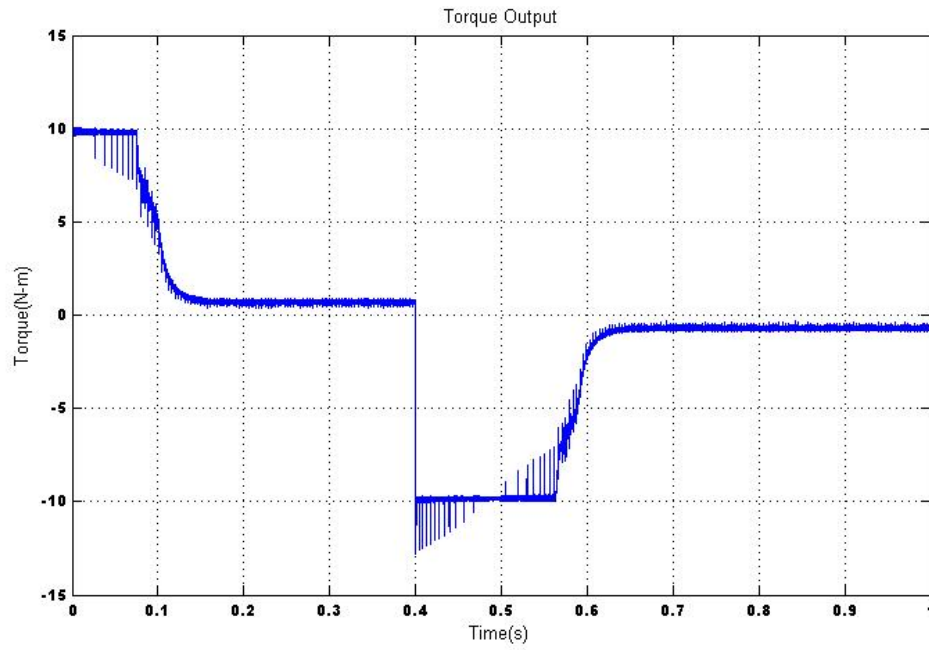


Fig 3.55 Electromagnetic Torque produced under speed reversal for FPCPI controller

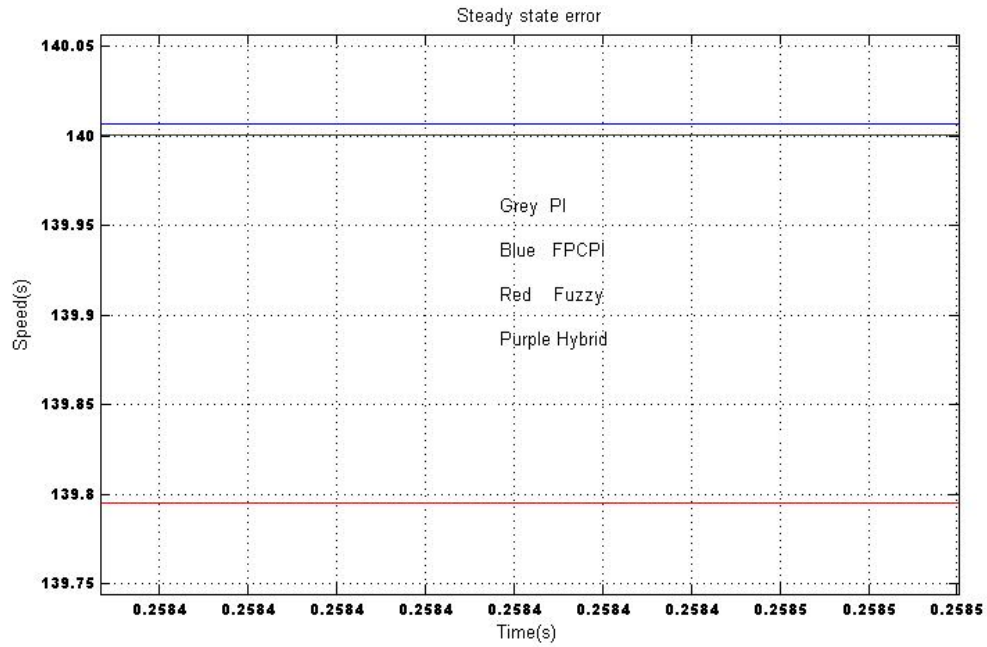


Fig 3.56 Steady State Error of controllers

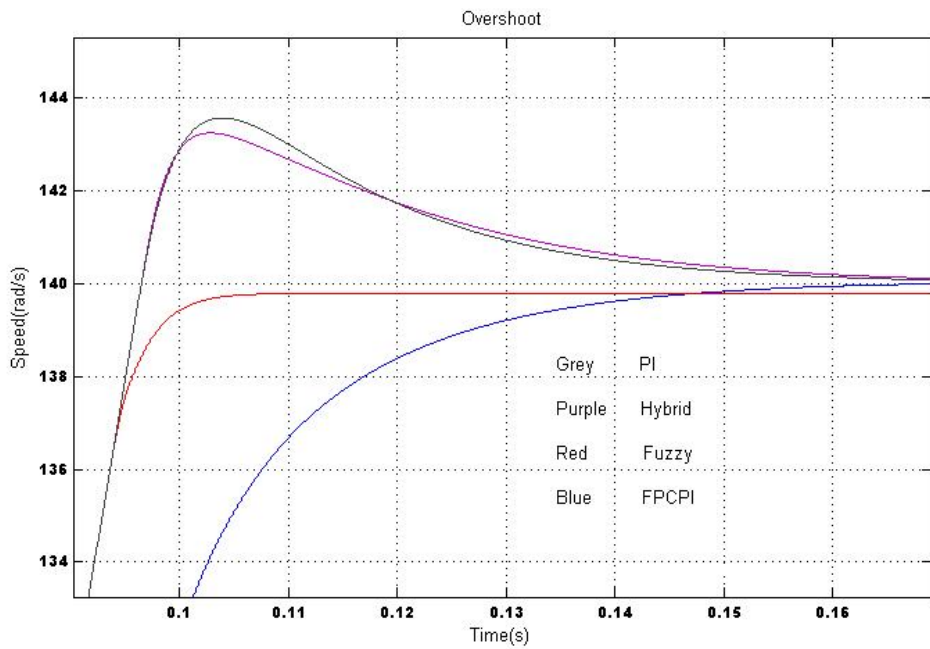


Fig 3.57 Starting Response of controllers

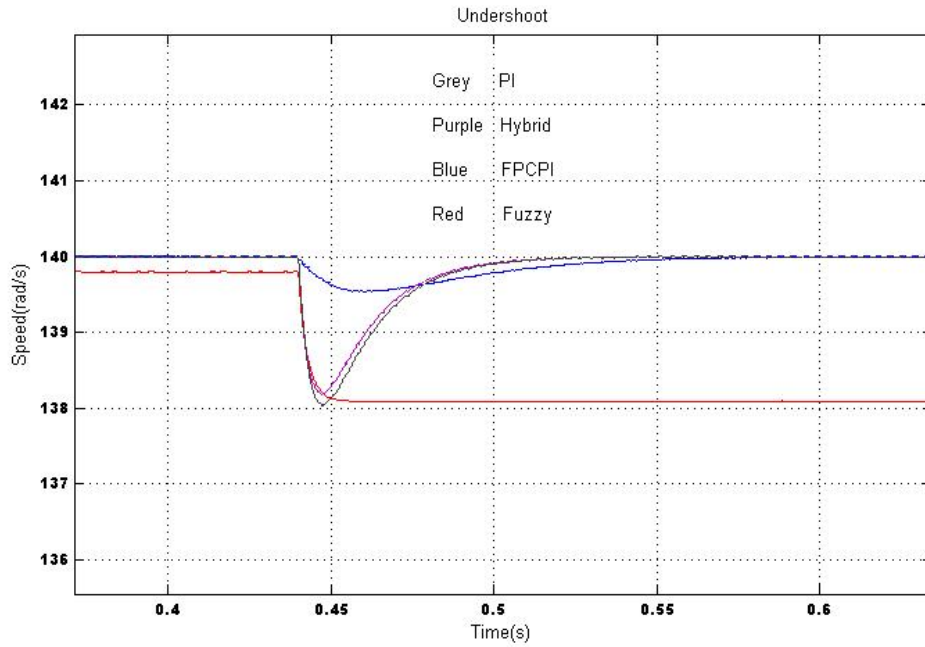


Fig 3.58 Undershoot on load application of controllers

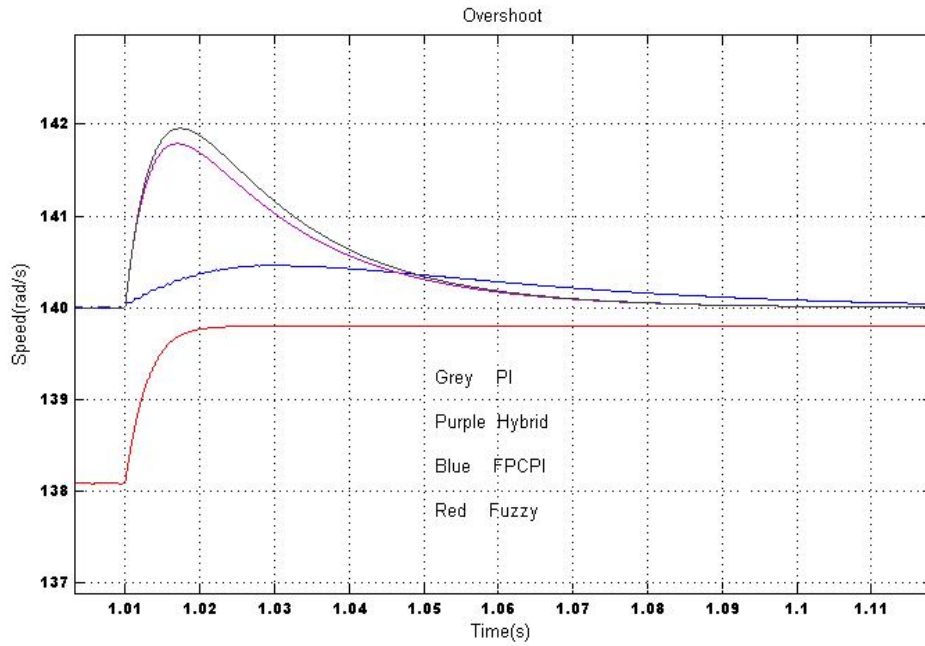


Fig 3.59 Overshoot on load removal of controllers

3.6.4 Comparative Study of Different Speed Controllers

The performance of a 2HP BLDC MOTOR drive has been simulated under various dynamic conditions namely, starting, speed reversal and load perturbation using the stated speed controller namely PI, Hybrid, FPPI and FI respectively. The obtained results are shown in the figures 3.17-3.24.

Table 3.3 shows that for the same reference speed PI, FPPI, Hybrid and FI speed controllers show a change in starting and reversal time respectively. Under no load conditions, the FL controller does show very low error but under loaded conditions the error is high. In order to take the advantages of PI and FL controllers and to eliminate the disadvantages of individual controllers, both the control techniques are combined and named as a hybrid speed controller. When the speed error is near to zero, the control is switched over to PI controller therefore eliminating disadvantage of steady state speed error of FI speed controller. When drive speed is away from the reference value, the control is changed over to FL controller, which provides improved dynamic performance.

The control action of PI, FI, and Hybrid and FPPI controllers is governed by the magnitude of deviation in rotor speed from the reference value. Instead of solely depending on the speed error, if FL controller is applied to modify the reference speed and the main control action uses the PI speed controller then

Table 3.4 Comparative Performance of Different Speed Controllers for 2 HP
 BLDC MOTOR Drive $\omega_r^* = 140$ rad/s, Reversal applied from $\omega_r^* = 140$ rad/s to
 $\omega_r^* = -140$ rad/s. at no-load , $T_l = 5$ N/m

Speed Controller	Starting Time(msecs)	Reversal Time(msec)	Speed Dip On load application (rad/s)	Speed rise On load removal(rad/s)	Steady State Error (rad/s) On no load
PI	181.7	276.1	2.0	2.0	0.0
HYBRID	180.6	273	1.8	1.8	0.0
FPCPI	161.6	250.4	0.5	0.5	0.0
FL	113.6	195	1.9	1.9	0.2

The Hybrid controller provides a good performance as it extracts the best of both the controllers. The FPPI controller also provides better performance than PI controller. The steady error incurred, when motor is started on load, can be observed in FL controller where as in FPPI and Hybrid controller error is quite low compared to FL controller. The PI controller requires vigorous retuning for different motors. The FPPI can provide a margin of insensitiveness to parameter variation.

3.7 CONCLUSIONS

The BLDC MOTOR drive has been mathematically modeled in MATLAB environment alongwith simulink and sim-powersystem toolboxes. The drive response has been simulated using the developed model under different operating conditions such as starting, speed reversal and load perturbation. A comparative study of different speed controllers for various operating condition has been made. The individual controllers have their own merits and demerits. Depending upon the application, a choice of controller can be made. When the requirement is that of simplicity and ease of application, the PI controller is to be good choice. When intelligence and fast dynamic response are important, then the FL technique may be selected. The main demerit in this option is the existence of steady state error on load application. To eliminate such a problem and to maintain the high level of performance in combination with fast dynamic response, the hybrid of FL and PI is better option. To make system insensitive to parameter variations, FPPI holds a better prospective.

CHAPTER IV

FUTURE SCOPE OF WORK

4.1 GENERAL

The main objective of the thesis has been aimed towards modeling of brushless DC motor drive, selection of appropriate controller for range of applications, implementation of BLDC MOTOR drive using fast speed, dedicated digital speed processor (DSP). Modeling and simulation of performance of the BLDC MOTOR drive under various operating closed loop speed controllers in MATLAB environment using simulink and simpowersystem blockset toolboxes, has been done and simulated results obtained has been found to be matching with design sheet provided by manufacture. Implementation of the BLDC MOTOR drive has been done by building various modules for it and testing of the drive prototype as whole to validate the developed model.

4.2 FURTHER SCOPE OF WORK

There are certain aspects which require further investigation; some of them are enlisted for investigations.

- 1) The reduction of sensors in BLDC MOTOR drive can further be investigated and implemented. The reduction in the number of sensors without any loss on quality of the signal estimated would lead to simplification of the controller, makes the controller more robust and reduce the overall cost of the drive system.
- 2) The PI controller is employed due to their lesser complexities and easy deployment. The tuning of the parameters of the controller is very rigorous. They

are very sensitive towards parameter variation and hence lesser robust. The investigations can be carried out using advanced techniques like neural network, fuzzy logic which can tune the parameters of the controller depending upon the operating conditions.

REFERENCES

- [1] T.J.E. Miller, *Brushless Permanent-Magnet and Reluctance Motor Drives*, Clarendon PRESS OXFORD, 1989.
- [2] R. Krishnan, *Electric Motor Drives Modeling, Analysis, and Control*, India Prentice-Hall 2002.
- [3] H. R. De Azevedo and K.P. Wong (SMIEEE), "A Fuzzy Logic Controller for Permanent Magnet Synchronous Machine a Sliding Mode Approach" in Proceedings of PCC-Yokohama 1993.
- [4] Nesimi Ertugrul and Paul Acamley "A New Algorithm for Sensorless Operation of Permanent Magnet Motors" in IEEE Transactions on Industry Applications", Vol. 30, No. 1, January February 1994.
- [5] Y. S. Jeon, H. S. Mok, G. H. Choe, D. K. Kim, and J.S. Ryu, "A New Simulation Model of BLDC MOTOR Motor With Real Back EMF Waveform" Dept. of Electrical Eng. Konkuk Univ., Komotek*, Jasontech** in 0-7803-6561-5/00/\$10.00 0 2000 IEEE.
- [6] Wook-Jin Lee and Seung-Ki Sul, "A New Starting Method of BLDC MOTOR Motors without Position Sensor".
- [7] Jianwen Shao, Member, IEEE,, Dennis Nolan, Maxime Teissier, and David Swanson, "A Novel Microcontroller-Based Sensorless Brushless DC (BLDC MOTOR) Motor Drive for Automotive Fuel Pumps in IEEE Transactions on Industry Applications, Vol. 39, No. 6, November / December 2003.
- [8] Jinyun Gan, C.C. Chan, K. T. Chau, and J. Z. Jiang , "Advanced Conduction Angle Control of Permanent Magnet Brushless Motor Drives" in 0-7803-4879-6/98/ 0 1998 IEEE.
- [9] Satoshi Ogasawara and Hirofumi Akagi, "An Approach to Position Sensorless Drive for Brushless dc Motors" in IEEE Transactions on Industry Applications, Vol. 27, No. 5, September October 1991.
- [10] S.D. Sudhoff and P.C. Krause, "Operating Modes of the Brushless DC Motor with a 120° Inverter" in IEEE Transactions on Energy Conversion Vol 5, No 3, September 1990.

- [11] Pragasen Pillay, Member, IEEE and Ramu Krishan, Member IEEE, "*Modeling, Simulation, and Analysis of Permanent-Magnet Motor Drives, Part 11: The Brushless DC Motor Drive*" in IEEE Transactions on Industry Applications Vol 25, No 2, March/April 1989.
- [12] Lee, Chung Yuen w0n, Member, IEEE, YOU Young Choe', "*Comparison of Characteristics Using two Hall-ICs and one Hall-IC for 3 phase Slotless FM Brushless DC Motor*" the 30th Annual Conference of the IEEE Industrial Electronics Society, November 2 - 6, 2004, Busan, Korea.
- [13] Z. Q. Zhu and Y. Liu, D. Howe, "*Comparison of Performance of Brushless DC Drives under Direct Torque Control and PWM Current Control*" Deptt of Electronic and Electrical Engineering, University of Sheffield, United Kingdom.
- [14] C. Bi, Z. J. Liu, and S. X. Chen, Member, IEEE, "*Estimation of Back-EMF of PM BLDC MOTOR Motors Using Derivative of FE Solutions*" in IEEE Transactions on Magnetics, Vol 36, No 4, July 2000.
- [15] Jianwen Shao and Dennis Nolan, "*Further Improvement of Direct Back EMF Detection for Sensorless Brushless DC (BLDC MOTOR) Motor Drives*" in STMICROELECTRONICS-POWER SYSTEM APPLICATIONS Lab 1375 E. Woodfield Rd, Suite 400 Schaumburg, IL 60173, USA.
- [16] Jianwen Shao, Dennis Nolan, and Thomas Hopkins, "*Improved Direct Back EMF Detection for Sensorless Brushless DC (BLDC MOTOR) Motor Drives*" in STMICROELECTRONICS-POWER SYSTEM APPLICATIONS Lab 1375 E. Woodfield Rd, Suite 400 Schaumburg, IL 60173, USA.
- [17] Nesimi Ertugrul, Member, IEEE, and Paul P. Acarnley, "*Indirect Rotor Position Sensing in Real Time for Brushless Permanent Magnet Motor Drives*" in IEEE Transactions on Power Electronics, Vol. 13, No. 4, July 1998.
- [18] Bhim Singh, B P Singh, (Ms) K Jain, "*Implementation of DSP Based Digital Speed Controller for Permanent Magnet Brushless dc Motor*" in IE (I) Journal-EL Vol 84, June 2003.
- [19] Thomas M. Jahns - IEEE, "*Motion Control with Permanent-Magnet AC Machines*" in Proceedings of the IEEE, Vol. 82. No. 8. August 1994.
- [20] Kuang-Yao Cheng, Shiu-Yung Lin, and Ying-Yu Tzou, "*On-Line Auto-Tuning of a DSP-Controlled BLDC MOTOR Servo Drive*" Power Electronics & Motion Control Lab. Department of Electrical and Control Engineering National Chiao Tung Univ., Taiwan, R.O.C.

- [21] Petar Crnosija, Toni Bjazic and R. Krishnan, "*Optimization of PM Brushless DC Motor Drive*" in ICIT 2003 - Maribor, Slovenia 2003 IEEE.
- [22] R. Krishnan, and Shiyong Lee, "*PM Brushless DC Motor Drive with a New Power-Converter Topology*" in IEEE Transaction on Industry Applications, Vol. 33, No. 4, July/August 1997.
- [23] C.C. Chan, W.Xia, J.Z. Jiang, K.T. Chau and M.L.Zhu, "*Permanent Magnet Brushless Drives*" in IEEE Industry Applications Magazine November/December 1998.
- [24] Seung-Jun Lee , Yong-Ho Yoon and Chung-Yuen Won, "*Precise Speed Control of the PM Brushless DC Motor for Sensorless Drives*" Dept. Information & Communication Eng., Sungkyunkwan University, Gyeonggi-do, Korea.
- [25] M.M. Salem, Yousry Alia, M.B. Zahran, and A.M. Zaki "*Real-Time Implementation of On-Line Trained Neuro-Controller for a BLDC MOTOR Motor*" Electronics Research Institute, Do&, Cairo, Egypt.
- [26] Paul P. Acarnley and John F. Watson IEEE, "*Review of Position-Sensorless Operation of Brushless Permanent-Magnet Machines*" IEEE Transactions on Industry Electronics, Vol. 53, No. 2, April 2006.
- [27] James P. Johnson M. Ehsani Yilcan Giizelgiinler, "*Review of Sensorless Methods for Brushless DC*" 1999 IEEE Power Electronics Laboratory, Texas A&M University, College Station, Texas.
- [28] Tae-Hyung Kim, Byung-Kuk Lee, and Mehrdad Ehsani, "*Sensorless Control of the BLDC MOTOR Motors From Near Zero to High Speed*" Texas A&M University, Dept. of Electrical Engineering College Station, TX 77843-3128, U.S.A 2003 IEEE.
- [29] Tae-Hyung Kim, and Mehrdad Ehsani, "*Sensorless Control of the BLDC MOTOR Motors From Near-Zero to High Speeds*" IEEE Transactions on Power Electronics, Vol. 19, No. 6, November 2004.
- [30] H.C.Chen and C.M.Liaw, "*Sensorless control via intelligent commutation tuning for brushless DC motor*" in IEEE Proc-Electr. Power Appl., Vol. 146, No. 6, November 1999.
- [31] Zhang Yan, Changxi Jin, and Vadim I. Utkin, "*Sensorless Sliding-Mode Control of Induction Motors*" in IEEE Transactions on Industrial Electronics, Vol. 47, No. 6, December 2000.

- [32] Ki-Hong Park, Tae-Sung Kim, Sung-Chan Ahn, Dong-Seok Hyun, “*Speed Control of High-Performance Brushless DC Motor Drives*” by Load Torque Estimation in Department of Electrical Engineering, HanYang University, HaengDang Dong, SungDong Gu, Seoul Korea ,2000 IEEE.
- [33] Genfu Zhou, Zhigan Wu, and Jianping Ying Unattenuated BEMF, “*Detection for Sensorless Brushless DC (BLDC MOTOR) Motor Drives*” at Delta Power Electronics Center 238 Miiixia Road, Caolu Industry Zone, Pudong, Shanghai, 201209, China.
- [34] Chuen Chien Lee, “*Fuzzy Logic in Control Systems: Fuzzy Logic Controller-Part I*” in IEEE Transactions On Systems, Man, and Cybernetics Vol.20,No.2 march/April,1990.
- [35] Chuen Chien Lee, “*Fuzzy Logic in Control Systems: Fuzzy Logic Controller-Part II*” in IEEE Transactions On Systems, Man, and Cybernetics Vol.20,No.2 march/April,1990.
- [36] Pierre Guillemin, “*Fuzzy Logic Applied to Motor Control*” in IEEE Transactions on Industry Applications, Vol. 32, No. 1, January /February 1996.
- [37] Jong-Hwan kim, Kwang-Choon and Edwin K.P. Chong, “*Fuzzy Precompensated PID Controllers*” IEEE Transactions on Control Systems Technology, Vol-2, No 4, December 1994
- [38] Martin Hellmann, “*Fuzzy Logic Introduction*” March 2001.
- [39] Bhim Singh, A.H.N.Reddy, S.S.Murthy, “*Hybrid Fuzzy Logic Proportional Plus Conventional Integral-Derivative Controller for Permanent Magnet Brushless DC Motor*” at Department of Electrical Engineering, Indian Institute of Technology, Delhi, India.
- [40] M.A.El-Sharkawi, A.A.El-Samahy, M.L.El-sayed, “*High Performance Drive of DC Brushless Motors Using Neural Network*” IEEE Transactions on Energy conversion, Vol 9, No.2, June 1994.

APPENDIX-I

The values of parameters of speed controllers considered in the investigation simulation analysis and the specifications of the motor are as follows:

Brushless DC motor:

Rating:	2.0 hp
Number of Poles:	4
Type of connection:	Star
Rated speed:	1500 rpm
Rated current:	4A
Resistance/phase:	2.8 Ω
Back EMF constant:	1.23V sec/rad
Inductance ($L_s + M$):	0.00521 H/phase
Moment of Inertia:	0.013 Kg-m ²
Proportional Constant:	1
Integral Constant:	50

BIO-DATA

- Name: Amarnath Yadav
- Date of Birth 13th March 1981
- Qualification Bachelor of Engineering, National
Institute of Technology, Surat, Gujarat
- Permanent address: 3-D Street-77, Sector-6, Bhilai
District-Durg, Chhattisgarh-490006